Improved and expanded Q-system reagents for genetic manipulations

Olena Riabinina[1], David Luginbuhl[2,3], Elizabeth Marr[1], Sha Liu[4], Mark N Wu[4], Liqun Luo[2,3] & Christopher J Potter[1]

The Q system is a repressible binary expression system for transgenic manipulations in living organisms. Through protein engineering and *in vivo* functional tests, we report here variants of the Q-system transcriptional activator, including QF2, for driving strong and ubiquitous expression in all *Drosophila* tissues. Our QF2, Gal4QF and LexAQF chimeric transcriptional activators substantially enrich the toolkit available for transgenic regulation in *Drosophila melanogaster*.

The characterization and manipulation of complex biological systems require sophisticated genetic tools. Binary expression systems are powerful in directing transgenic expression of effector genes. In *Drosophila*, the Gal4-UAS[1] system has been widely adopted, but it has limitations. Existing Gal4 expression patterns are often too broad and require refinement, and Gal4-UAS alone is insufficient for independent manipulation of two distinct populations of cells. Two additional binary expression systems have been developed: the λ phage LexA-LexAop[2] and the Q system, derived from the *qa* gene cluster of the fungus *Neurospora crassa*[3]. The Q system comprises the transcriptional activator QF, the QF effector *QUAS*, the QF suppressor QS and the nontoxic drug quinic acid, which inhibits QS. Thus, in addition to QF being repressible like Gal4, the Q system has the advantage that expression can be temporally regulated by quinic acid.

Despite its immediate application[4–8], the original QF was lethal when expressed broadly *in vivo*[3], which made it impossible to obtain flies that expressed QF under the control of either strong pan-neuronal or ubiquitous promoters. The cause of this toxicity was unknown. To address this problem, we aimed to identify the region of QF that was responsible for toxicity and to generate a QF variant that retained full activity yet could be broadly expressed with no adverse effects. For our experimental approach, we created chimeric proteins between QF, Gal4 and/or LexA[2]. Previous studies[9,10], together with our bioinformatic alignments of QF and Gal4, predicted that QF is structurally similar to Gal4 (refs. 11–14). We hypothesized that, like Gal4 (ref. 15), QF can be subdivided into three domains (**Fig. 1a**) that perform specific and independent functions: the DNA-binding and dimerization domain (DBD) containing a Zn_2-Cys_6 motif that recognizes and binds to *UAS* or *QUAS* sites; a middle domain (MD) that has no clear function but that might be involved in endogenous regulation or stability; and a transcriptional activation domain (AD) that recruits molecular machinery necessary for transcription and that also binds the Gal80 or QS suppressor.

To overcome limitations of the original QF, any new QF variant should be capable of generating healthy transgenic flies when broadly expressed. In addition, it should exhibit strong transcriptional activity yet remain QS suppressible. We generated a series of constructs in which certain QF domains were modified (**Fig. 1a** and **Supplementary Fig. 1a**). In Gal4QF, $QF2^{w(eaker)}$ and QF_e, the QF AD was mutated to reduce activity by altering the charge on the C terminus. In QF2, $QF2^w$ and LexAQF, the QF MD was completely removed; in $QF_{f–i}$, the QF MD was partially removed. Finally, in Gal4QF, LexAQF, $QF_{a–d}$ and $QF_{j–l}$, the QF DBD or QF AD were swapped for analogous Gal4 or LexA domains. To quantitatively measure activity levels, we performed luciferase assays in cultured *Drosophila* Schneider 2 (S2) cells (**Fig. 1b**). To assay for QF toxicity, we attempted to generate transgenic animals expressing each construct under the pan-neuronal *neuronal Synaptobrevin* (*nSyb*; hereafter, *nsyb*) promoter (**Fig. 1**, **Supplementary Fig. 1** and **Supplementary Table 1**). To allow direct comparison between transgenic constructs that use the same enhancer activation sequence (*UAS*, *QUAS* or *LexAop*), we used the PhiC31 integrase system and targeted all transgenic insertions to the same attP2 genomic landing site (3L: 68A4). However, direct comparison between transgenic factors using different activation sequences, e.g., *UAS* reporters (**Fig. 1c**) versus *QUAS* reporters (**Fig. 1d**), cannot be made owing to differing activities of the reporters.

In relative luciferase activity assays and *in vivo* expression analyses, the optimal QF variants exhibited high activity levels (**Fig. 1b–f** and **Supplementary Table 1**), were efficiently repressed by QS (**Supplementary Table 1**) and produced healthy transgenic animals. We initially hypothesized that a potent QF AD may be the source of toxicity as it may be squelching cellular transcription factor components[16], but QF variants that contained the original (QF2 and LexAQF) and mutated AD of QF ($QF2^w$ and Gal4QF) were not toxic. Instead, constructs containing the MD of QF either failed to produce transgenic animals (QF_d and QF_g, **Supplementary Fig. 1**) or were extremely unhealthy (QF_f), thereby implicating the QF MD as the major source of QF toxicity. Deletion of this domain yielded two smaller QF variants, QF2 and $QF2^w$, which exhibited strong but differing QF activities

[1]The Solomon H. Snyder Department of Neuroscience, Johns Hopkins University School of Medicine, Baltimore, Maryland, USA. [2]Howard Hughes Medical Institute, Stanford University, Stanford, California, USA. [3]Department of Biology, Stanford University, Stanford, California, USA. [4]Department of Neurology, Johns Hopkins University School of Medicine, Baltimore, Maryland, USA. Correspondence should be addressed to C.J.P. (cpotter@jhmi.edu).

RECEIVED 16 DECEMBER 2013; ACCEPTED 1 DECEMBER 2014; PUBLISHED ONLINE 12 JANUARY 2015; DOI:10.1038/NMETH.3250

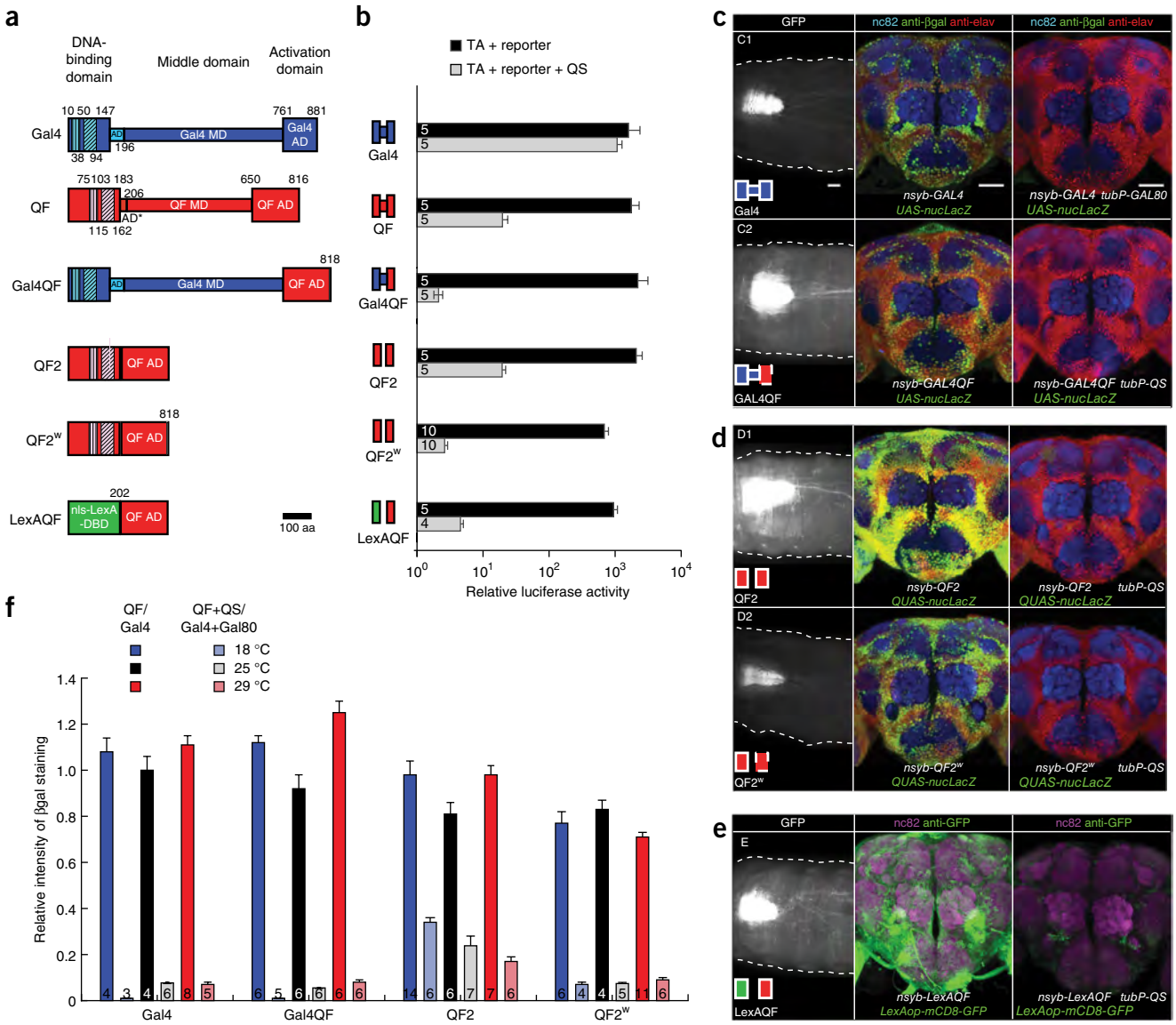

Figure 1 | Activity of modified QF transcriptional activators *in vitro* and *in vivo*. (**a**) Schematics of Gal4, original QF (ref. 3) and four new transcriptional activators. DBD, DNA-binding domain; MD, middle domain; AD, activation domain. Vertical hatching indicates Zn_2-Cys_6 zinc-finger motifs, diagonal hatchings mark dimerization domains. Numbers indicate amino acid position. Constructs are drawn to scale. (**b**) The transcriptional activity (black) and QS repression (gray) of QF transcriptional activators (TA) in S2 cells. Numbers in bars indicate the number of independent repeats. (**c**–**e**) Pan-neuronal *in vivo* expression of constructs driven by *neuronal Synaptobrevin* (*nsyb*) promoter at 25 °C. Left columns, mCD8-GFP expression in third instar larvae (representative of $n = 4$–6; scale bar, 100 µm); center columns, nuclear LacZ expression in adult *Drosophila* brain (representative of $n = 4$–6; scale bar, 50 µm); right columns, Gal80- or QS-induced suppression of LacZ expression in adult brains (representative of $n = 5$–7; scale bar, 50 µm). Brains were immunostained for elav (red), LacZ (green; βgal, β-galactosidase) and nc82 (blue). (**e**) Larval and adult expression of mCD8-GFP driven by *nsyb-LexAQF* construct (representative of $n = 5$). Right panel, *tubP-QS* suppression of LexAQF activity (representative of $n = 5$). (**f**) LacZ expression, quantified as described in Online Methods. Numbers in bars indicate the number of brains for each condition. Error bars, s.e.m.

in vitro (2,089 ± 477 s.e.m. and 685 ± 44 s.e.m. times above control, respectively; $P = 0.00064$; Kolmogorov-Smirnov test) and *in vivo* (**Fig. 1c**–**e** and **Supplementary Fig. 1c**). Both QF2 and QF2^w were capable of generating healthy pan-neuronally expressing transgenic animals. Thus, the QF MD is dispensable for full QF activity, yet it is the major source of QF toxicity *in vivo*.

We assessed expression patterns and strength of the transactivators at 18 °C, 25 °C and 29 °C with both membrane-tagged GFP (**Supplementary Fig. 2**) and nuclear LacZ reporters (**Fig. 1f**). In findings similar to the *in vitro* results (**Fig. 1b**), QF2, QF2^w, Gal4QF and LexAQF had activity levels comparable to that of Gal4 and could be robustly repressed by QS at all tested temperatures. In agreement with Mondal *et al.*[17], we found that Gal4 activity did not vary with temperature. This contrasts with the temperature dependence often observed with many GAL4 enhancer traps[18], which likely reflects the use of temperature-sensitive elements in these constructs[1].

We quantified the expression level for $LexA_{BD}$:QF_{AD} chimeric proteins (LexAQF and QF_l) with only a GFP reporter (**Fig. 1e** and **Supplementary Figs. 1d** and **2**), as *LexAop-nuc-lacZ* reporter lines were not available. Both constructs drive strong expression *in vivo*, and pan-neuronally expressing transgenic animals were healthy.

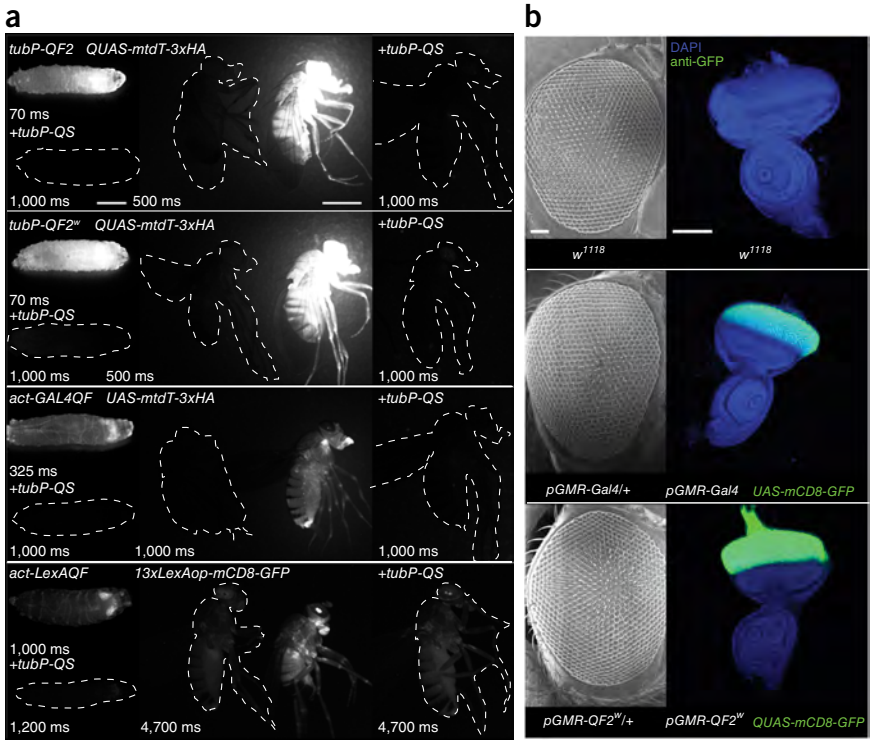

Figure 2 | *In vivo* expression driven by *tubulin*, *actin* and *GMR* promoters. (**a**) Ubiquitous expression of GFP or membrane-targeted tandem dimer Tomato (mtdT) reporters in third instar larvae (left; representative of $n = 4–6$) and in adult flies (right column; representative of $n = 5$). Larvae carry a *tubulin* or *actin* driver line and an mtdTomato or mCD8-GFP reporter as well as a *tubP-QS* transgene where indicated. Adult flies (center) are imaged next to the controls (left) that bear only the TA or only effector transgenes (dashed white outline). The rightmost subpanels (marked by "*+tubP-QS*") show flies that, in addition to the indicated driver and reporter transgenes, also carry *tubP-QS*. Expression of *act-LexAQF* driver is visualized with an mCD8-GFP reporter. Imaging settings were identical for all images, apart from the duration of exposure, which is indicated for each image. Scale bars, 1 mm. (**b**) Scanning electron micrographs of the adult female eyes (left; representative of $n = 10$) and GFP expression in the eye-antennal imaginal disc (right; representative of $n = 5$) for flies of the indicated genotypes. Scale bars, 50 µm.

Expression levels of LexAQF-driven GFP were similar to those of Gal4-driven GFP at 18 °C, 25 °C and 29 °C (**Supplementary Fig. 2**) and could be repressed by QS at all temperatures (data not shown). The LexAQF chimeras offer a useful alternative to LexA:VP16 and LexAGal4 transcriptional activators[2] in that LexAQF chimeras are independent of the Gal4-UAS system and can be reversibly suppressed by QS (**Fig. 1e** and **Supplementary Fig. 1d**).

The *nuc-lacZ* quantification of QS-suppressed activity of QF2 *in vivo* (**Fig. 1f**) suggested that a number of cells were still weakly labeled and detectable by our algorithm. To further validate the ability of QS to functionally inhibit QF2 and QF2^w, we performed whole-animal rescue experiments. We drove the expression of the temperature-sensitive endocytotic recycling protein encoded by *shibire* (at 29 °C) with *nsyb-QF2 or nsyb-QF2^w*, which did not result in surviving adults, as expected. This lethality was fully rescued in flies that also carried a *tubulin-QS* transgene (**Supplementary Table 2**), indicating that QF2 and QF2^w are efficiently suppressed by QS *in vivo*. In addition, the activity of all QF AD variants (QF2, QF2^w, Gal4QF and LexAQF) could be regulated by feeding quinic acid to larvae or adult flies (**Supplementary Fig. 3**). Quinic acid had a stronger effect on peripheral receptor neurons than on central brain neurons, presumably reflecting differential exposure of the neurons to quinic acid.

The new transactivators (QF2, QF2^w, Gal4QF and LexAQF), together with Gal4, offer the possibility of using Gal4, LexA and Q systems simultaneously in overlapping subsets of cells. We verified that activity of any two of these transactivators in the same cells did not result in toxicity or reporter silencing effects by generating all possible binary combinations of the *nsyb* transactivator flies (**Supplementary Fig. 4**).

To test whether expression of the new transactivators might cause toxicity in non-neuronal tissues, we generated flies that express QF2, QF2^w, Gal4QF and LexAQF under the control of the ubiquitous promoters *tubulin* (*alphaTub84B*) and *actin* (*act5C*). These flies were viable, and activity of the transactivators was robust in late embryos (data not shown), larvae and adult flies (**Fig. 2a**). These ubiquitous drivers could be effectively suppressed by QS in the whole larvae or adult flies (**Fig. 2a** and **Supplementary Fig. 5**). Examination of imaginal discs (epithelial tissue) and larval body walls (muscle) (**Supplementary Fig. 5a**,**b**) confirmed the broad transactivator expression patterns of QF2, QF2^w, Gal4QF and LexAQF.

Evidence that Gal4, when driven at very high levels, could be toxic to the fly was first found in experiments using the strong synthetic eye promoter pGMR[19,20]. *pGMR-QF2^w* transgenic animals exhibited strong QF-induced GFP expression in the eye-antennal imaginal disc (**Fig. 2b**), yet they had no morphological eye defects at the adult stage. These results suggest that QF2^w, even when very strongly expressed, was not toxic to the cell.

As a final readout of QF2 and QF2^w effects *in vivo*, we examined three different behaviors in flies pan-neuronally expressing *QF2*, *QF2^w* or *GAL4* in the same *w^{1118}* genetic background (**Fig. 3** and **Supplementary Table 3**). Behaviors are a sensitive measure of *in vivo* health: they require key processes, such as development, neuronal wiring and neuronal function, to be unaffected. The *nsyb-QF2* and *nsyb-QF2^w* flies were indistinguishable from *nsyb-GAL4* controls in olfactory attraction to apple cider vinegar and humidified air, but they were slightly but significantly ($P = 0.0275$ and $P = 0.0302$, respectively) less repelled by CO_2 gas than the controls (**Fig. 3a**). *nsyb-QF2* and *nsyb-QF2^w* flies exhibited phototactic responses comparable to those of *nsyb-GAL4* flies and wild-type controls (**Fig. 3b**). In locomotor activity assays (**Fig. 3c–f**), daily activity and daily sleep amounts were not significantly different ($P > 0.05$) between *nsyb-QF2*, *nsyb-QF2^w* and control flies. Both *nsyb-QF2* and *nsyb-QF2^w* flies

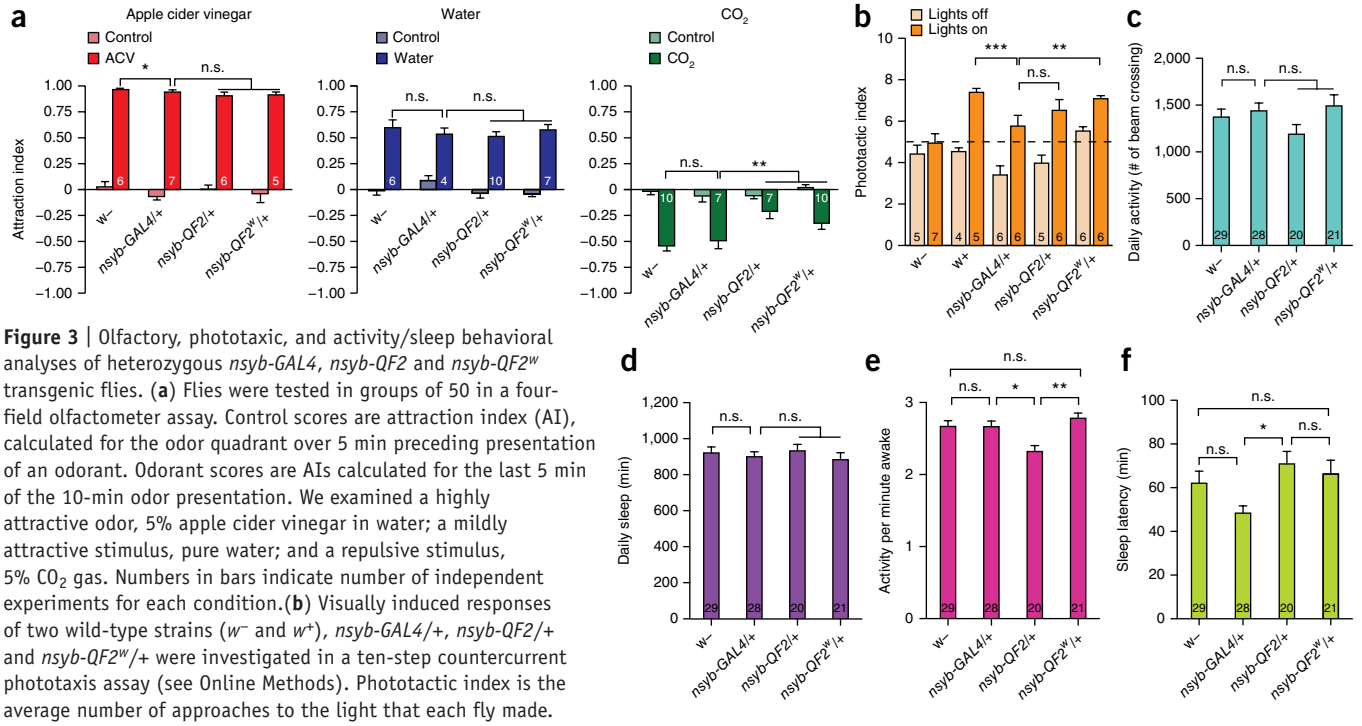

Figure 3 | Olfactory, phototaxic, and activity/sleep behavioral analyses of heterozygous *nsyb-GAL4*, *nsyb-QF2* and *nsyb-QF2^{w}* transgenic flies. (**a**) Flies were tested in groups of 50 in a four-field olfactometer assay. Control scores are attraction index (AI), calculated for the odor quadrant over 5 min preceding presentation of an odorant. Odorant scores are AIs calculated for the last 5 min of the 10-min odor presentation. We examined a highly attractive odor, 5% apple cider vinegar in water; a mildly attractive stimulus, pure water; and a repulsive stimulus, 5% CO_2 gas. Numbers in bars indicate number of independent experiments for each condition.(**b**) Visually induced responses of two wild-type strains (w^- and w^+), *nsyb-GAL4/+*, *nsyb-QF2/+* and *nsyb-QF2^{w}/+* were investigated in a ten-step countercurrent phototaxis assay (see Online Methods). Phototactic index is the average number of approaches to the light that each fly made. Numbers in bars indicate number of independent experiments for each condition. (**c**–**f**) Daily activity (**c**), daily sleep time (**d**), waking activity (**e**) and sleep latency (**f**) for w^- (n = 29 flies), *nsyb-GAL4/+* (n = 28), *nsyb-QF2/+* (n = 20) and *nsyb-QF2^{w}/+* (n = 21) flies, assayed as outlined in the Online Methods. Error bars, s.e.m. $*P < 0.05$, $**P < 0.01$, $***P < 0.001$; as determined by the nonparametric Kolmogorov-Smirnov test. n.s., not significant.

exhibited normal circadian rhythms under constant darkness (**Supplementary Table 3**). Taken together, these results demonstrate that pan-neuronal expression of *QF2* and *QF2^{w}* is compatible with proper neuronal development and function.

In summary, we have developed two next-generation versions of QF—QF2 and QF2^{w}—that have dramatically reduced toxicity and can be expressed broadly *in vivo*. QF2 is best suited when strong transcriptional activity is required in subsets of cells. QF2^{w} is optimal for broad expression patterns or strong promoters. We have also developed chimeric Gal4QF and LexAQF transactivators which, while still activating *UAS-geneX* and *LexAop-geneX* effectors respectively, are QS suppressible, quinic acid regulatable and Gal80-insensitive. These transactivators substantially expand the range of possible applications of the Q system by itself as well as in combination with Gal4-UAS and LexA-LexAop for intersectional targeting.

METHODS

Methods and any associated references are available in the online version of the paper.

Note: Any Supplementary Information and Source Data files are available in the online version of the paper.

ACKNOWLEDGMENTS

We thank S. Djuranovic (Johns Hopkins University), A. Radhakrishnan and A. Schuller for S2 cells and training in S2 cell culturing and luciferase assays, B. Smith for help with scanning electron microscopy, T. Shelley for manufacturing the olfactometer setup, J. Simpson (Janelia Farm Research Campus) for an *n-Synaptobrevin* promoter containing construct, and C.-C. Lin, B. Akitake, R. Reed and Center for Sensory Biology members for discussions and suggestions. This work was supported by grants from the Whitehall Foundation (C.J.P.), US National Institutes of Health (R01DC013070, C.J.P.; R01NS079584, M.N.W., R01 DC005982, L.L.) and Howard Hughes Medical Institute (L.L.).

AUTHOR CONTRIBUTIONS

C.J.P. and O.R. conceived of the project and designed most of the experiments. S.L. and M.N.W. designed the daily activity and sleep tests. O.R., E.M., S.L. and C.J.P. performed the experiments. D.L. performed embryo injections and generated most of the transgenic animals. L.L. provided reagents and suggestions. O.R. and C.J.P. wrote the manuscript with feedback from all authors.

COMPETING FINANCIAL INTERESTS

The authors declare no competing financial interests.

1. Brand, A.H. & Perrimon, N. *Development* **118**, 401–415 (1993).
2. Lai, S.-L. & Lee, T. *Nat. Neurosci.* **9**, 703–709 (2006).
3. Potter, C.J., Tasic, B., Russler, E.V., Liang, L. & Luo, L. *Cell* **141**, 536–548 (2010).
4. Silies, M. *et al. Neuron* **79**, 111–127 (2013).
5. Pérez-Garijo, A., Fuchs, Y. & Steller, H. *eLife* **2**, e01004 (2013).
6. Mann, K., Gordon, M.D. & Scott, K. *Neuron* **79**, 754–765 (2013).
7. Wei, X., Potter, C.J., Luo, L. & Shen, K. *Nat. Methods* **9**, 391–395 (2012).
8. Gohl, D.M. *et al. Nat. Methods* **8**, 231–237 (2011).
9. Tsuji, G. *et al. Mol. Microbiol.* **38**, 940–954 (2000).
10. Baum, J.A., Geever, R. & Giles, N.H. *Mol. Cell. Biol.* **7**, 1256–1266 (1987).
11. Hidalgo, P. *et al. Genes Dev.* **15**, 1007–1020 (2001).
12. Walters, K.J., Dayie, K.T., Reece, R.J., Ptashne, M. & Wagner, G. *Nat. Struct. Mol. Biol.* **4**, 744–750 (1997).
13. Kraulis, P.J., Raine, A.R.C., Gadhavi, P.L. & Laue, E.D. *Nature* **356**, 448–450 (1992).
14. Marmorstein, R., Carey, M., Ptashne, M. & Harrison, S.C. *Nature* **356**, 408–414 (1992).
15. Ma, J. & Ptashne, M. *Cell* **48**, 847–853 (1987).
16. Gill, G. & Ptashne, M. *Nature* **334**, 721–724 (1988).
17. Mondal, K. *et al. J. Mol. Biol.* **370**, 939–950 (2007).
18. Wilder, E.L. & Perrimon, N. *Development* **121**, 477–488 (1995).
19. Freeman, M. *Cell* **87**, 651–660 (1996).
20. Kramer, J.M. & Staveley, B.E. *Genet. Mol. Res.* **2**, 43–47 (2003).

ONLINE METHODS

Bioinformatics of QF. Phyre2 (ref. 21) was used for bioinformatic prediction of QF secondary protein structures and disordered regions to guide domain borders for deletion or chimeric protein constructs. The QF dimerization domain at amino acids 115–162 was predicted based on protein alignments with Gal4 (ref. 22) and Phyre2 predictions of a coiled-coil secondary structure. An internal QF AD was predicted based on protein alignments with Gal4 and charge plots[15] that indicate a negatively charged basic region at amino acids 182–206. The QF $Zn(II)_2Cys_6$ binuclear DNA-binding domain at amino acids 75–103 was as predicted in ref. 9. The QF AD was predicted as in Wei *et al.*[7]. An InterProScan[23] of QF predicted a conserved fungal transcription factor domain at amino acids 372–465, which was the basis for construct QF_i.

Toxicity of transgenic QF constructs. Several constructs were generated as detailed below that failed to produce transgenic animals despite multiple attempts (>1,000 embryo injections per construct).

Pan-neuronal *Synaptobrevin* promoter (*nsyb*) constructs that failed to produce transgenic animals included *nsyb-QF* in a *piggyBac* transformation vector for random genomic insertions (*pXL-BACII-nsyb-QF-hsp70*) and *nsyb-QF* in an *attB* vector directed to *attP2* (*pattB-nsyb-QF-hsp70*).

The following pan-tissue constructs that used the tubulin promoter (*tubP*) failed to produce transgenic animals: *tubulin P-QFcodon_deoptimzed* (cdo), in a *piggyBac* transformation vector (*pXL-BAC-tubulinP-QFcdo*); *tubulinP-QF::QF2AD^{weak}*, in a *piggyBac* transformation vector that contains the same AD mutant as in *QF2^{w}* but with full-length *QF* (*pXL-BAC-tubulinP-QF2M1*); and *tubulinP-QF::QF$_e$AD*, in a *piggyBac* transformation vector that contains the same AD mutant as in *QF$_e$* but with full-length *QF* (*pXL-BAC-tubulinP-QF2M2*).

Note that *nsyb-QFcdo*, in a *piggyBac* transformation vector for random genomic insertions, was able to generate transgenic animals. Of the ten original lines, induced *QUAS-mCD8GFP* activity was weak, and none of the lines exhibited pan-neuronal expression. In addition, as we were unable to generate *tubulinP-QFcdo* transgenic animals, *QFcdo* constructs were not characterized further.

Our initial hypothesis was that the QF AD was the major source of QF toxicity. To circumvent this toxicity when generating *QF* transgenic animals, we injected constructs into flies containing a *tubP-QS* transgenic background. However, this did not help yield transgenic animals. Our recent findings suggest this is likely due to the MD of *QF* being the major source of toxicity, which would not be attenuated by *QS* expression. Nonetheless, transgenic animals containing the Gal4 binding domain and QF AD (QF_b, **Supplementary Fig. 1**) demonstrated the strongest activity of all the constructs and were not as healthy as the same QF chimera (Gal4QF, **Fig. 1**) containing the QF2^{w} AD. This suggests that a fully potent QF AD might, in some instances, contribute toward *in vivo* toxicity. We note that even Gal4 can be toxic when expressed at high levels[16,19].

Recombinant DNA construction. Plasmids were constructed by standard procedures including enzyme digestions, PCR and subcloning. Some of the plasmids were manufactured using the In-Fusion HD Cloning System (Clontech, Cat #639645). Plasmid inserts were verified by DNA sequencing. Apart from the constructs used in the reported experiments, we describe four additional constructs (*pPT-QF2-hsp70*, *pattB-DSCP-QF2-hsp70, pattB-hsp70-QF2-hsp70, pCasper-QF2-hsp70*) that may be useful for creating new *QF2* lines. Primer sequences are shown in **Supplementary Table 4**.

QF codon variants. *QFrco, QF recodonized.* The original QF sequence from Neurospora often yielded tracheal expression in enhancer-trap constructs[3]. This was likely due to a cryptic tracheal enhancer in the QF gene sequence. To eliminate this tracheal enhancer, the entire coding region of QF was recodonized (DNA2.0, Inc.) by manually choosing codons expected to yield average expression (http://www.kazusa.or.jp/codon/cgi-bin/showcodon.cgi?species=7227). Transgenic flies expressing QFrco enhancer traps no longer exhibited background tracheal expression (data not shown).

QFcdo, QF codon-deoptimized. A *Drosophila* codon deoptimized variant of *QF* led to reduced expression levels in transgenic constructs (data not shown). *QFcdo* enhancer trap flies induced weak reporter activity and also no longer exhibited tracheal expression.

Chimeric and deletion cloning strategy. Chimeric constructs and deletions were generated by a multistep PCR process using a high-fidelity Taq polymerase (Phusion Taq, NEB). PCR fragments were generated that had terminal regions of sequence overlap (typically 17–25 base pairs to achieve a predicted T_m of 62–65 °C) to other PCR fragments. The overlapping PCR fragments were used in a second round of PCR in which the overlapping PCR fragments each acted as primers for PCR amplification. After five cycles, additional oligos were included to selectively amplify full-length PCR products. All constructs were sequence verified before generating transgenic animals. All *pattB-nsyb-geneX-hsp70* constructs were generated by inserting an EcoRI/AatII digested PCR product (Gal4, QF_a-QF_e, GAL4QF) or In-Fusion compatible PCR product (QF2, QF2^{w}, QF_f-QF_k, LexAQF, LexAG4QF) into the EcoRI/AatII site of *QF*-excised *pattB-nsyb-QF-hsp70*. Chimera construction details are listed in **Supplementary Table 5**.

S2 cell culture constructs. *pAC-QF$_x$ (Addgene #46089–46105).* These plasmids contain QF_x variants under the control of the *actin5c* promoter for expression in S2 cell culture. The vector backbone for these constructs was obtained by digesting the *pAC-QF* plasmid[3] with BamHI and NotI to remove the *QF* gene. New *QF* variants were PCR amplified from corresponding *pattB-QF$_x$* plasmids and ligated into the vector backbone by an In-Fusion reaction. For PCR amplification, the same forward primer was used for all QF variants in combination with Gal4 DNA-binding domain (IF_FOR_GAL4DBD), QF DNA-binding domain (IF_FOR_QFDBD) and LexA binding domain (IF_FOR_LEXADBD) primers. Likewise, the same reverse primer was used to PCR-amplify constructs with a Gal4 AD (IF_REV_GAL4AD) or an original QF AD (IF_REV_QFAD). Constructs with the LexA binding domain were amplified with reverse primer IF_REV_LEXADBD. The reverse primers for the following were GAL4QF, IF_REV_GAL4QF; QF2^{w}, IF_REV_QF2W; QF_f, IF_REV_QF_F.

p-LexAop-Luc2. This construct allows expression of the firefly luciferase reporter under the control of LexAop in S2 cell culture experiments. The vector backbone was obtained by

cutting *pQUAS-luc2* (ref. 3) with HindIII to remove *QUAS*. 5x LexAop was PCR-amplified from *pJFRC19-13XLexAop2-IVS-myr::GFP*[24] (Addgene Plasmid #26224) with forward primer IF_FOR_LexAOP_LUC and reverse primer IF_REV_LexAOP_LUC, and sub-cloned by an In-Fusion reaction.

Additional constructs used for generating transgenic animals. *pCasper4-tubP-QF2-hsp70 (Addgene #46127).* This construct was used to generate fly lines with random genomic insertions of the *tubulinP-QF2* transgene. The vector backbone was obtained by cutting *pCasper4-tubP-GAL80* (ref. 25) with NotI and XhoI. The *QF2-hsp70_terminator* insert was PCR amplified from the *pattB-QF2* plasmid with forward primer IF_FOR_TUB_QF2 and reverse primer IF_REV_TUB_QF2, and cloned into the digested vector by an In-Fusion reaction.

pCasper-act(B)-QF2^{w}-hsp70. This plasmid was used to generate fly lines with random genomic insertions of the *actin-QF2^{w}* transgene. Transgenic flies are not described in this paper owing to the availability of a stronger ubiquitous driver line, obtained with *pCasper-tubP-QF2w-hsp70*, but are available upon request. *pCasper-act(B)* (DGRC stock#1068) was digested with EcoRI and PstI, *QF2-hsp70* was PCR amplified from *pattB-nsyb-QF2* with forward primer IF_FOR_ACT_QF2W and reverse primer IF_REV_ACT_QF2W and cloned into the digested vector by an In-Fusion reaction.

pCasper-tubP-QF2^{w}-hsp70 (Addgene #46128). The 371-bp terminus of *QF2^{w}* was excised from *pattB-nsyb-QF2w-hsp70* by digestion with NheI/XhoI and cloned into *pCasper4-tubulinP-QF2-hsp70* in which the *QF2* C terminus had been excised by NheI/XhoI digestion.

pCasper-act-GAL4QF. This construct was used to generate transgenic flies with random genomic insertions of the actin-GAL4QF transgene. pCasper-act(B)-QF2^{w}-hsp70 was digested with BamHI and NotI to remove QF2w-hsp70_terminator fragment. The GAL4QF-hsp70_terminator fragment was PCR amplified from 5-pattB-synaptobrevin-G4BDDM-QFADM1-hsp70 with the forward primer IF_FOR_ACT_GAL4QF and reverse primer IF_REV_ACT_GAL4QF and subcloned into the cut pCasper-act vector by an In-Fusion reaction.

pCasper-act-LexAQF. This construct was used to generate transgenic flies with random genomic insertions of the actin-GAL4QF transgene. pCasper-act(B)-QF2^{w}-hsp70 was digested with BamHI and NotI to remove QF2w-hsp70_terminator fragment. The LexAQF-hsp70_terminator fragment was PCR amplified from pattB-synaptobrevin-14-LexA-QF-hsp70 with the forward primer IF_FOR_ACT_LEXAQF and reverse primer IF_REV_ACT_LEXAQF and subcloned into the cut pCasper-act vector by an In-Fusion reaction.

pGMR-QF2^{w}(Addgene #46130). This plasmid was used to generate random genomic insertions of *QF2^{w}*, driven by the strong *GMR* eye-specific promoter[19,20]. Vector *pGMR-GAL4* was digested with EcoRI to remove the *GAL4* gene, and *QF2^{w}* was PCR amplified from *pAC-QF2^{w}* with forward primer IF_FOR_GMR_QF2W and reverse primer IF_REV_GMR_QF2W, and subcloned into the digested *pGMR* vector by an In-Fusion reaction.

Additional plasmids generated for QF2. *pCasper-act(B)-QF2^{w}-act_term (Addgene #46126).* *QF2^{w}* was excised from *pAC-QF2w* by digestion with BamHI/NotI and ligated into *pCasper4-actin5cB-QF2* digested with BamHI/NotI to excise *QF2*.

pPT-QF2-hsp70 (Addgene #46136). Vector *pPTGAL*[26] was digested with PstI, and *QF2-hsp70* PCR amplified from *pattB-hsp70-QF2-hsp70* with forward primer IF_FOR_PPT_QF2 and reverse primer IF_REV_PPT_QF2 and subcloned into the digested vector by an In-Fusion reaction. This construct contains a minimal *hsp70* promoter and allows for convenient subcloning of enhancers upstream of *QF2*.

pattB-DSCP-QF2-hsp70 (Addgene #46133). The *pattb-QF-hsp70* plasmid[3] and *pattb-syb-QF2* were both cut with EcoRI and ZraI, and the isolated *QF2* insert was ligated into the digested *pattb-hsp70* vector using the Rapid DNA Ligation Kit (Roche). The *pattb-QF2-hsp70* plasmid was digested with EcoRI and BamHI, and the *DSCP* promoter PCR amplified from *pattB-DSCP-QF-SV40* (ref. 3) with forward primer IF_FOR_DSCP_QF2 and reverse primer IF_REV_DSCP_QF2, and cloned into the digest vector by an In-Fusion reaction. This PhiC31 integrase compatible plasmid utilizes the *DSCP* promoter[27] to allow for the cloning of enhancer regions to drive *QF2* expression.

pattB-hsp70P-QF2-hsp70T (Addgene #46134). The *pattb-QF2-hsp70* plasmid was digested with EcoRI and BamHI, and the *hsp70* promoter PCR amplified from *pUAST*[1] with forward primer IF_FOR_ATTB_QF2 and reverse primer IF_REV_ATTB_QF2, and subcloned into the digested vector by an In-Fusion reaction. This PhiC31 integrase compatible plasmid utilizes the *hsp70* minimal promoter to allow for the cloning of enhancer regions to drive *QF2* expression.

pCasper-act(B)-QF2-act_term (Addgene #46125). *QF2* was PCR amplified from *pattB-nsyb-QF2* using oligos IF-FOR-pCasper-ActB-QF7 and IF-REV-pCaspActB-QF7 and In-Fusion (Clontech) cloned into *pCasper-act(B)* digested with BamHI.

pCasper4-QF2-hsp70 (Addgene #46135). The *QF2-hsp70* cassette was PCR amplified from *pattB-nsyb-QF2-hsp70* to include flanking XbaI restriction sites and inserted into the XbaI site of *pCasper4* (DGRC stock# 1213).

Progenitor plasmids for constructs described in this paper. *pattB-synaptobrevin-QFcdo-hsp70.* The *Synaptobrevin* promoter was PCR amplified from *pattB-nsyb-DSCP-QF-SV40* to include flanking BamHI and EcoRI restriction sites. The tubulin promoter from *pattB-tubulinP-QFcdo-hsp70* was excised by digestion with BamHI/EcoRI and replaced with the digested *n-Synaptobrevin* PCR product.

pattB-nsyb-DSCP-QF-SV40. The *n-Synaptobrevin* promoter was PCR amplified from the plasmid *pPTGAL4+n-syb* (a vector containing the *n-Synaptobrevin* promoter upstream of the *CMV* minimal promoter, kindly provided by J. Simpson, Janelia Farm Research Campus) to include flanking EcoRI restriction sites. The EcoRI digested PCR product was ligated into the EcoRI restriction site of *pattB-DSCP-QF*[3].

pattB-tubulinP-QFcdo-hsp70. The hsp70 terminator from *pXN-QF-hsp70* was PCR amplified to include AscI/NotI restriction sites (hsp70-AscI-FOR, hsp70-NotI-REV) and ligated into the *pattB-tubulinP-QFcdo-SV40* vector digested with AscI/NotI to excise the SV40 terminator.

pattB-tubulinP-QFcdo-SV40. QFcdo was excised from *p35030-QFcdo* (synthesized by DNA2.0) by digestion with EcoRI/AscI

doi:10.1038/nmeth.3250

and replaced by ligation the QF in plasmid *pattB-tubulinP-QF+AscI* digested with EcoRI/AscI.

pattB-tubulinP-QF+AscI. The tubulin promoter from *pCasper-tubulinP-GAL80* (ref. 25) was excised by digestion with BamHI/EcoRI and ligated into the BamHI/EcoRI site of the *pattB-QF+AscI* plasmid.

pattB-QF+AscI. An AscI restriction site between QF and the SV40 terminator was introduced into *pattB-QF-SV40* (ref. 3) by digestion with AatII and ligation of a compatible sticky-ended annealed dsDNA of target sequence TGGCGCGCCA.

pattB-synaptobrevin-QF-hsp70. The *n-Synaptobrevin* promoter was PCR amplified from *pattB-nsyb-QF-SV40* to include BamHI and EcoRI restriction sites and ligated into the BamHI/EcoRI multiple-cloning site of *pattB-QF-hsp70* (ref. 3).

pattB-tubulinP-QFrco-hsp70. The *QFcdo-hsp70* fragment from *pattB-tubP-QFcdo-hsp70* was excised by EcoRI/XhoI digestion and replaced with an EcoRI/XhoI *QFrco-hsp70* cassette digested from *pXL-BAC-attP-Ppromoter-QFrco-hsp70*.

pXL-BAC-attP-Promoter-QFrco-hsp70. *pJ241-QFrco* (synthesized by DNA2.0) was digested with SnaBI/BglII to excise *QFrco* and ligated into the SnaBI/BglII site of *pXL-BAC-LoxP-DsRed-LoxP-attP-Promoter-QF-hsp70* in which *QF* had been excised by digestion with SnaBI/BglII.

pXL-BAC-tubulinP-QFrco-M1(EQ->KK). The C terminus of *QFrco* was mutated by PCR-amplifying *QFrco* from *pXL-BAC-tubulinP-QFrco-hsp70* using primers *QFrco-NheI-FOR*, *QFrcoM1-REV*, digestion with NheI/BglII and ligation into NheI/BglII digested *pXL-BAC-tubulinP-QFrco-hsp70*.

pXL-BAC-tubulin-QFrco-M2(E->K). The C terminus of *QFrco* was mutated by PCR-amplifying *QFrco* from *pXL-BAC-tubulinP-QFrco-hsp70* using primers *QFrco-NheI-FOR*, *QFrcoM2-REV*, digestion with NheI/BglII and ligation into NheI/BglII digested *pXL-BAC-tubulinP-QFrco-hsp70*.

***Drosophila* genetics.** Flies were kept on a standard fly medium with a 12:12 h light/dark (LD) cycle in a 25 °C incubator, unless indicated otherwise. *UAS*, *QUAS* and *LexAop* reporter lines were obtained from the Bloomington *Drosophila* Stock Center (NIH P40OD018537). Reporter transgenes were integrated at various genomic positions, but where possible, we used the same reporter line with new transactivator driver lines to compare activation strengths. Standard procedures were used to generate transgenic *Drosophila* either by P-element or *piggyBac* transgenesis or by PhiC31 integration[3].

Quinic acid experiments. To investigate the effect of quinic acid (QA), we used 2- to 3-d female flies of one of the following genotypes: (i) *tub-QS/+; nsyb-QF2, QUAS-mCD8:GFP/+*, (ii) *tub-QS/+; nsyb-QF2^{w}, QUAS-mCD8:GFP/+*, (iii) *tub-QS/+; nsyb-GAL4QF, UAS-mCD8:GFP/+* or (iv) *tub-QS/+; nsyb-LexAQF, LexAop-IVS-myr:GFP/+*.

These flies were raised on standard fly medium until they were 2- to 3-d-old adults, at which point they were transferred into vials containing 10 ml of 1% agarose (Denville Scientific, Cat #CA3510-8) supplemented with 0.1 g of sucrose (Sigma, Cat #S0389) and 0.6 g of QA (Sigma, Cat #138622). The vials also contained yeast paste made from dry yeast and QA solution (3 g of QA per 10 ml of H_2O, neutralized to pH 6.5 by 10 mM NaOH solution). The same QA solution was used to moisten a Kimwipe that was embedded into the agarose gel. Flies were kept in these QA-containing vials for 3 d, after which brains were dissected and immunostained as described below.

S2 cell transfections and luciferase assays. S2 cells (Life Technologies, Cat #R690-07) were cultured in Express Five SFM (serum-free medium, Gibco, Cat #10486-025), supplemented with 18 mM L-glutamine (Gibco, Cat #25030-081) and penicillin/streptomycin/L-glutamine mixture (25,000 units/25,000 µg/200 mM, Lonza, Cat #17-718R, 4.5 ml per 1 liter of SFM). The cells were maintained in 75-cm^2 tissue culture flasks (Sarstedt, Cat #83.1811.002) at room temperature and atmospheric CO_2, and passaged every 4–6 d for no more than 26 generations. Cells were tested for mycoplasma infection by a PCR reaction using primers specific to 16S mycoplasma ribosomal RNA coding regions. For transfections, 0.3 ml per well of cell-containing medium and 0.3 ml per well of fresh medium were placed into 24-well plates (Corning, Cat #3524) 24 h before transfection. All transfections were performed using Effectene Transfection Reagent (Qiagen, Cat #301425). 200 ng of DNA (per well) were mixed with Effectene reagent, enhancer and buffer according to manufacturer's instructions, supplemented with 0.4 ml (per well) of fresh medium and carefully pipetted into the wells. For QF_x activity assays, each well was transfected with 12.5 ng of a transcription factor *pAC-QF$_x$* plasmid, 50 ng of firefly luciferase reporter plasmid (*pLexAop-luc2*, *pQUAS-luc2*, or *pUAS-luc2*), 50 ng of *Renilla* luciferase plasmid (*pAC-hRluc*) for normalization and 87.5 ng of *pBluescript* (*pBS-KS*) plasmid. In the controls, 12.5 ng of the transcription factor plasmid were replaced by 12.5 ng of *pBluescript*. We always transfected one of the wells in each 24-well plate with 200 ng of *pBluescript* and left one well untransfected for control purposes. For QS repression assays, 87.5 ng of *pBluescript* were replaced by 87.5 ng of *pAC-QS* plasmid and cotransfected with *pAC-QF$_x$*, firefly and *Renilla* luciferase plasmids. Controls for QS assays were the same as for QF activity assays (firefly and *Renilla* reporters and *pBluescript* plasmid). Cells were lysed 48 h after transfection by replacing the medium in the wells with 0.1 ml of passive lysis buffer (PLB) from the Dual Luciferase Reporter Assay System (Promega, Cat #E1980) and shaking the plates at room temperature for 10 min. For luciferase activity measurements, the original lysates were diluted 10,000 times in PLB and analyzed by a Fluorostar Optima (BMG Labtech) plate reader immediately after lysing. Each lysate sample was placed into three different wells in a 96-well plate; from each well the luminescence was measured automatically six times (once per second) after the addition of firefly luciferase substrate and six times (once per second) after the addition of *Renilla* luciferase substrate. The relative luminescence (RL) of each well was calculated as

$$\mathrm{RL} = \frac{\overline{\mathrm{Firefly\_measurement}_{3-6}}}{\overline{\mathit{Renilla}\_\mathrm{measurement}_{3-6}}}$$

where $\overline{X}$ is the average luminescence signal in response to luciferase X substrate. The average was calculated for measurements 3–6 because the first two measurements were often substantially different from the following four. To obtain the relative luciferase activity (RLA, **Fig. 1b**), the RL was averaged between the three wells that contained the same lysate. Next, this average RL, calculated

for wells with transcription factor, was divided by a control RL, obtained from a corresponding control wells (only reporter plasmids without transcription factor).

$$\mathrm{RLA} = \frac{\overline{\mathrm{RL}_{\mathrm{transcription\_factor}}}}{\overline{\mathrm{RL}_{\mathrm{no\_transcription\_factor}}}}$$

For example, for *pAC-GAL4* plasmid

$$\mathrm{RLA}_{\mathrm{Gal4}} = \frac{\overline{\mathrm{RL}_{\mathrm{pAC-Gal4}}}}{\overline{\mathrm{RL}_{\mathrm{pUAS-luc2}}}} = \frac{\dfrac{\overline{\mathrm{Firefly\_measurement}_{3-6,\mathrm{pAC-Gal4}}}}{\overline{\mathit{Renilla}\_\mathrm{measurement}_{3-6,\mathrm{pAC-Gal4}}}}}{\dfrac{\overline{\mathrm{Firefly\_measurement}_{3-6,\mathrm{pUAS-luc2}}}}{\overline{\mathit{Renilla}\_\mathrm{measurement}_{3-6,\mathrm{pUAS-luc2}}}}}$$

and for *pAC-QF* plasmid

$$\mathrm{RLA}_{\mathrm{QF}} = \frac{\overline{\mathrm{RL}_{\mathrm{pAC\text{-}QF}}}}{\overline{\mathrm{RL}_{\mathrm{pQUAS\text{-}luc2}}}} = \frac{\dfrac{\overline{\mathrm{Firefly\_measurement}_{3-6,\mathrm{pAC-QF}}}}{\overline{\mathit{Renilla}\_\mathrm{measurement}_{3-6,\mathrm{pAC-QF}}}}}{\dfrac{\overline{\mathrm{Firefly\_measurement}_{3-6,\mathrm{pQUAS-luc2}}}}{\overline{\mathit{Renilla}\_\mathrm{measurement}_{3-6,\mathrm{pQUAS-luc2}}}}}$$

Thus, one RLA measurement was obtained for each of the wells from the original 24-well plate that contained a transcription factor plasmid. **Figure 1b** shows the results of four or five RLA measurements for each construct, apart from *pAC-QF2*^{w}, which was measured ten times. Each RLA measurement was obtained from independent transfections performed on different days.

Immunohistochemistry. Dissection of larval imaginal discs and adult brains, immunostaining and confocal imaging were done as described previously[28]. In short, brains of third instar larvae or 4- to 5-d-old adult flies were dissected in PBS, fixed for 20 min at room temperature, washed at room temperature in PBT for 5–6 h, blocked in 5% NGS in PBT and placed in primary antibody mixes for three nights at 4 °C. Next, the brains were washed for several hours in PBT at room temperature and placed in secondary antibodies mix for two nights at 4 °C. The following day the brains were washed in PBT and placed in mounting solution (Slow Fade Gold) overnight at 4 °C, and mounted on a microscope slide the next day. To visualize GFP expression, we used rabbit anti-GFP (Life Technologies #A11122, 1:100), chicken anti-GFP (Aves Labs Inc., #GFP1020, 1:250) and mouse nc82 (DSHB, 1:25; not used for larval brains) primary antibodies; for LacZ experiments we used preabsorbed rabbit anti–β-galactosidase (MP Biomedicals #08559762, 1:50), Rat-ELAV-7E8A10 anti-ELAV (DSHB, 1:50) and mouse nc82 (1:25) primary antibodies; to visualize mtdT-3HA, we used rat anti-HA (Roche #11867423001) primary antibody (1:100). Secondary antibodies used for GFP expression were Alexa 488 anti-rabbit (Invitrogen #A11034, 1:200) and Cy3 anti-mouse (Jackson ImmunoResearch #115-165-062, 1:200). For LacZ experiments: Cy3 anti-rabbit (Jackson ImmunoResearch #111-165-144, 1:200), 633 anti-rat (Invitrogen #A21094, 1:200) and Alexa 488 anti-mouse (Invitrogen #A11029, 1:200). For mtdT-3HA experiments: Cy3 anti-rat (Jackson ImmunoResearch #112-165-167, 1:200). Larval imaginal discs were stained in DAPI (1:100) for 10 min during one of the PBT washes after secondary antibody incubation.

Whole-animal imaging. Third instar larvae were placed on a small metal plate on top of crushed ice or on a temperature-controlled plate and imaged by a Zeiss SteREO DiscoveryV8 microscope equipped with a GFP-470 and ds-Red filters and a Jenoptik ProgRes MF cool CCD camera. Monochrome images were acquired in ProgRes Mac Capture Pro 2.7 software and stored in .tif format. Adult flies (3–5 d old) were anesthetized on a CO_2 pad and imaged as described for larvae. Images that are compared to each other were obtained under identical hardware and software settings.

Confocal imaging and image processing. Brains were imaged on an LSM 700 Zeiss confocal microscope equipped with a LCI Plan-Neofluar 25×/0.8 Imm Korr DIC M27 water-immersion objective, at 512 × 512 pixel resolution, with 1-µm or 2.37-µm *z* steps. See **Supplementary Note** for details. Zen 2012 Release Version 8 software was used for image acquisition. Microscope settings were kept the same for the genotypes that were later compared to each other, i.e., all *nsyb-QF$_x$/(Q)UAS-mcd8-GFP* brains, all *nsyb-QF$_x$/(Q)UAS-nucLacZ* brains, etc.

For illustration purposes, confocal images were processed in ImageJ to collapse *z* stacks into a single image using maximum-intensity projection and to pseudocolor different acquisition channels using an RGB Merge plug-in. No other image processing was performed on the confocal data.

To quantify LacZ expression, we used a custom-written Matlab (MathWorks) script. The script (**Fig. 1f**) identified cells in the elav channel and used the outlines of these cells as a mask to select the corresponding pixels in the LacZ channel. Then it calculated the average intensity of these pixels in the LacZ channel and normalized it by the average intensity of initially selected elav cells. The algorithm for identifying cells was adapted from a script by T. Kuo and J. Buyn (Center for Bioimage Informatics, also used in ref. 3). The cells were identified for every image in a *z* stack, and the intensity measures of each image were averaged to produce one number per brain.

To quantify GFP expression (**Supplementary Fig. 2**), we identified pixels with above-threshold intensity in the GFP channel on each image of a *z* stack. Next, we calculated the average intensity of the identified pixels, producing one number per imaged brain. Finally, we averaged the intensity measures of separate brains.

Scanning electron microscopy imaging. Heads of 3- to 5-d-old female flies were mounted without any processing onto aluminum stubs with double-stick carbon tape (Ted Pella) or Blu-Tack (Bostik). Images were acquired at 200× magnification with a Leo 1530 field emission scanning electron microscope operating at 1 kV.

Behavioral tests. All flies used in behavioral tests were outcrossed to the same wild-type *isoD1 white*$^{-}$ background for five generations. Control and experimental data sets were compared using the nonparametric Kolmogorov-Smirnov test.

doi:10.1038/nmeth.3250

Phototactic behavior. Experiments were conducted in a photography dark room using overhead infrared lights for illumination. The F15T8/WW fluorescent lamp light source was switched off during control experiments. 50 male and 50 female 5-d-old flies were used for each experiment. Prior to the assay, flies were kept in vials with regular fly medium at room temperature. The experimental setup was as described previously[29] and consisted of 21 cell culture tubes (14 ml, BD Falcon, REF 352059), arranged in two rows of 10 and 11 tubes so that the open ends of the tubes were facing each other. For example, tube 0 was opposite tube 0′, tube 1 was opposite tube 1′ and so on. Flies were initially placed in tube 0 and given 2 min to walk toward the light source and into tube 0′. Next, tube 0′ was shifted into register with tube 1, the flies were tapped down from tube 0′ into tube 1 and again given 2 min to walk toward the light and into tube 1′ and so on. In total, each fly had ten chances to walk toward the light source in the course on an experiment. The phototaxis index (PI) was calculated as

$$\mathrm{PI} = \frac{\sum_{i=0}^{10} i * N_i}{\sum_{i=0}^{10} N_i}, \mathrm{PI} \in [0;10]$$

where N_i is the number of flies in tube i at the end of the experiment. PI equals to the average number of times a fly walked toward the light source, with a PI = 10 indicating that all flies always walked toward the light and PI = 0 meaning that no flies walked toward the light. We repeated the experiment and the lights-off control 4–7 times for each genotype. **Figure 3b** represents the data as an average PI for each genotype and experimental condition; error bars show s.e.m.

Activity and sleep assays. For activity/sleep measurements, flies were outcrossed five times into iso31 background (Bloomington #5905). Flies were entrained to a 12:12 h LD cycle for at least 2 d before being assayed. Flies were kept in glass tubes containing 5% sucrose and 2% agar, and monitored using the *Drosophila* Activity Monitoring System (Trikinetics). Activity counts from 4- to 7-d-old female flies were collected in 1-min bins in the LD cycle at 25 °C for 2 d. Activity/sleep parameters were computed using Matlab-based custom software. Sleep was identified as periods of inactivity lasting at least 5 min. For circadian behavior measurement, activity counts were recorded in 30-min bins in constant darkness over a 6-d period and analyzed using ClockLab (Actimetrics). Period length (τ) was determined by χ^2 periodogram analysis, and rhythm strength was measured by relative FFT, calculated by fast Fourier transform analysis.

Olfactory behaviors in the four-field assay. These olfactory experiments were conducted as described previously[30]. The experimental setup consisted of a temperature-controlled light-proof chamber (45 cm × 27 cm × 49 cm) that was equipped with four air inlets, a CCD camera (Sony CCD IR XC-E150 with Pentax 12.5mm 1:1.4 TV lens) and two arrays of infrared LEDs. The chamber was designed to accommodate a rectangular arena (23 cm × 23 cm × 3 cm), the corners of which could be connected to the four air inlets. The arena consisted of a Teflon base sandwiched between two glass plates. The bottom glass plate had a hole (diameter = 6 mm) in the middle to let out the air that was pumped into the arena from the corners. The arena was placed horizontally inside the chamber and filmed by a CCD camera from above. The video data were acquired at 30 f.p.s., 640 × 480 pixels, by a custom-written GUI. Immediately after acquisition, the data were processed by custom-written Matlab scripts and stored as a .mat file. The data structure contained information about coordinates of each detected fly at each point in time, and also about trajectories of individual flies, whenever the trajectories could be resolved unequivocally.

25 female and 25 male flies were starved for 41–43 h before each experiment and were 5 d old when tested. The flies were transferred without anesthesia into the four-field arena that was immediately placed into the experimental setup and flushed with clean dry air (DA) at 0.1 l/min from each corner for 20 min. We recorded the flies' activity for 10 min in DA and for the following 10 min with 5% CO_2, water vapor, or 5% apple cider vinegar in water blown into one quadrant of the arena. Three other quadrants were flushed with DA at all times. Experiments were conducted in the dark, at 25 °C maintained in the experimental chamber. Flies' activities were quantified as an attraction index (AI) calculated for the odorant quadrant. The 10-min DA recording served as a control for the odor experiment. If the flies' activity was too low or they were distributed unevenly in the arena (|AI|>0.15) during the 10-min DA recording, this group of flies was not tested with an odorant. The AI was calculated as

$$\mathrm{AI} = \frac{N_{\mathrm{odorant}} - \overline{N_{\mathrm{DA}}}}{N_{\mathrm{odorant}} + \overline{N_{\mathrm{DA}}}}, \mathrm{AI} \in [-1;1]$$

where N_{odorant} is the number of data points in the odorant quadrant during 10 min, and $\overline{N_{\mathrm{DA}}}$ is the average number of data points in the other three quadrants that were always flushed with DA. Each walking fly generated 30 data points per second. A fly was deemed stationary if its speed was consistently below 4.5 pixel/s for 3.3 s. The data points from stationary flies were discarded. AI = −1 corresponds to complete repulsion from the odor quadrant, and AI = 1 corresponds to complete attraction toward the odor quadrant.

Code availability. Custom-written Matlab scripts, used for quantifying confocal imaging data and for behavioral analyses, are available upon request.

Reproducibility. Our sample size (**Fig. 3**) is similar to that normally used in the literature for these kinds of experiments. No data were excluded from the analysis. No randomization was used, and no blinding was used.

21. Kelley, L.A. & Sternberg, M.J.E. *Nat. Protoc.* **4**, 363–371 (2009).
22. Zhang, L., Bermingham-McDonogh, O., Turcotte, B. & Guarente, L. *Proc. Natl. Acad. Sci. USA* **90**, 2851–2855 (1993).
23. Zdobnov, E.M. & Apweiler, R. *Bioinformatics* **17**, 847–848 (2001).
24. Pfeiffer, B.D. *et al. Genetics* **186**, 735–755 (2010).
25. Lee, T. & Luo, L. *Neuron* **22**, 451–461 (1999).
26. Sharma, Y., Cheung, U., Larsen, E.W. & Eberl, D.F. *Genesis* **34**, 115–118 (2002).
27. Pfeiffer, B.D. *et al. Proc. Natl. Acad. Sci. USA* **105**, 9715–9720 (2008).
28. Wu, J.S. & Luo, L. *Nat. Protoc.* **1**, 2110–2115 (2006).
29. Benzer, S. *Proc. Natl. Acad. Sci. USA* **58**, 1112–1119 (1967).
30. Gao, X.J. *et al. Curr. Biol.* **23**, 1163–1172 (2013).

Supplementary Figure 1

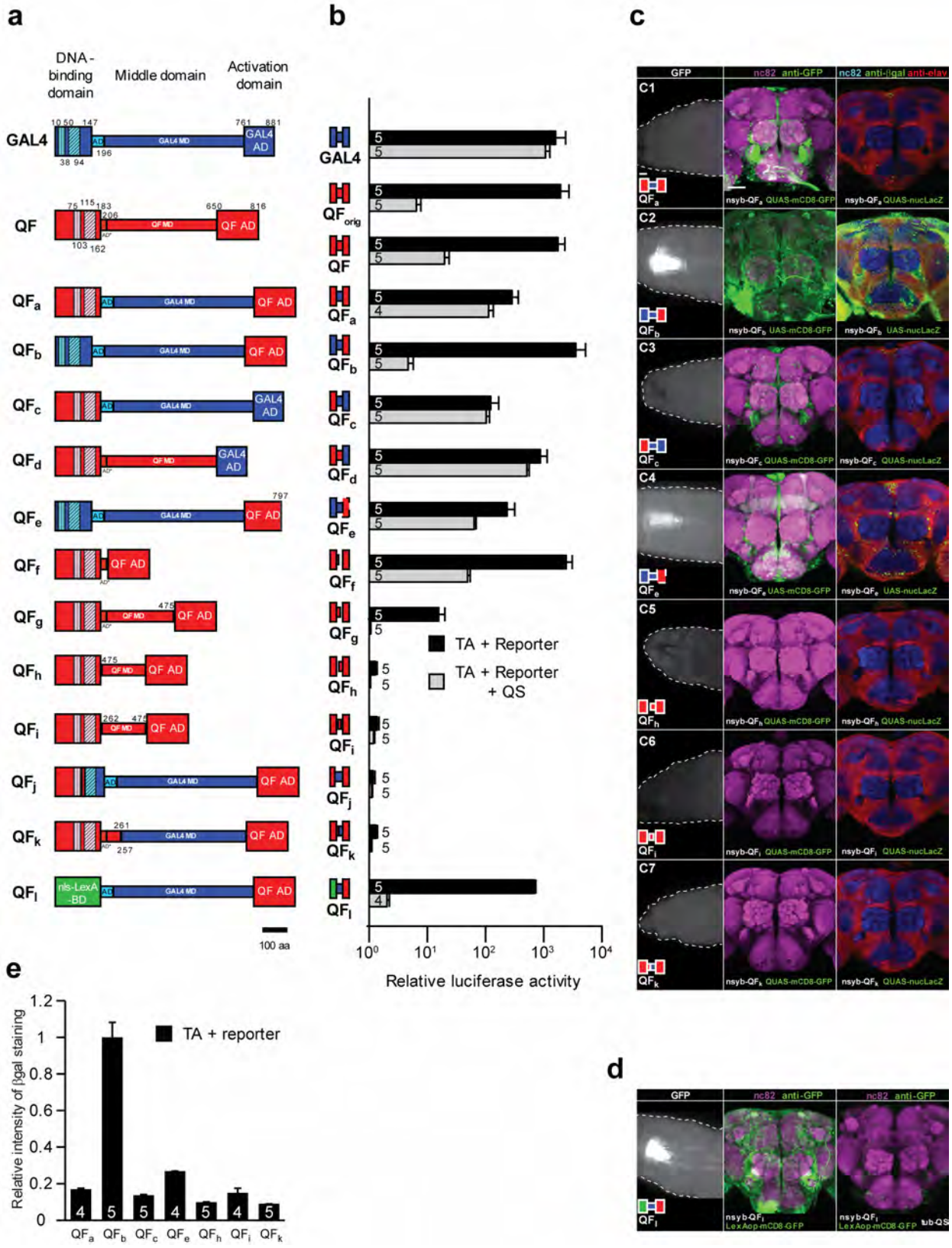

Nature Methods: doi:10.1038/nmeth.3250

Supplementary Figure 1

***In vitro* and *in vivo* activities of additional QF variants**.

This figure characterises the additional QF variants generated to find the region responsible for QF toxicity. Some variants yielded insufficient transcriptional activity ($QF_{a,c,e,g-k}$), some were either lethal in vivo (QF_d), or exhibited substantial (QF_f) or slight (QF_b) in vivo toxicity. QF_l is an efficient and non-toxic LexAQF chimera, but since a smaller and stronger alternative exists (LexAQF, **Fig. 1**) that showed similar activity, QF_l was not characterized further. **(a)** Schematics of GAL4, QF and twelve experimental transcriptional activators. BD, DNA binding domain; MD, middle domain; AD, activation domain. Vertical hatching indicates Zn2-Cys6 zinc finger motifs, diagonal hatchings mark dimerization domains. Numbers indicate amino acid position. Constructs are drawn to the same scale. Construct QF_b is structurally identical to GAL4QF (**Fig. 1**), apart from 4 amino acid changes in the C-terminus of the protein (see **Online Methods**). Construct QF_e was made by replacing the C-terminal 22 amino acids of QF with four lysines. This change also likely affected the QS binding site. **(b)** The transcriptional activity (black bars) of QF variants were investigated by transfecting S2 cells with *actin-QF_X* plasmid, firefly luciferase reporter plasmid (*pLexAop-luc2*, *pQUAS-luc2* or *pUAS-luc2*), *Renilla* luciferase plasmid (*pAC-hRluc*) for normalization, and *pBluescript* (*pBS-KS*) plasmid for loading control. For QS repression assays (grey bars), *Bluescript* plasmid was replaced with *pAC-QS* plasmid and co-transfected together with *actin-QF_X*, firefly and *Renilla* luciferase plasmids. *QF_{orig}* is the original Neurospora QF codon sequence from Ref.. *QF* in this table, and for all variants, has been re-codonized to yield average *Drosophila* expression levels (see **Online methods**). Numbers in bars indicate the number of independent repeats. Error bars are SEM. Luciferase activity is shown on a log scale. **(c)** Pan-neuronal in vivo expression of constructs driven by neuronal *synaptobrevin* (*nsyb*) promoter at 25 ˚C. Left column shows mCD8-GFP expression in third-instar larvae (scale bar, 100 µm), middle column shows mCD8-GFP expression in adult brain (nc82, magenta; GFP, green; scale bar, 50 µm), and the right column nuclear lacZ expression in adult brains (elav, red; lacZ, green; nc82, blue). **(d)** Larval and adult expression of *LexAop-mCD8:GFP*, driven by the *nsyb-QF_l* construct. Right panel, *tub-QS* suppression of QF_l activity. **(e)** Quantification of LacZ expression (see **Online Methods**). Numbers in bars indicate the number of brains for each condition. Error bars are SEM.

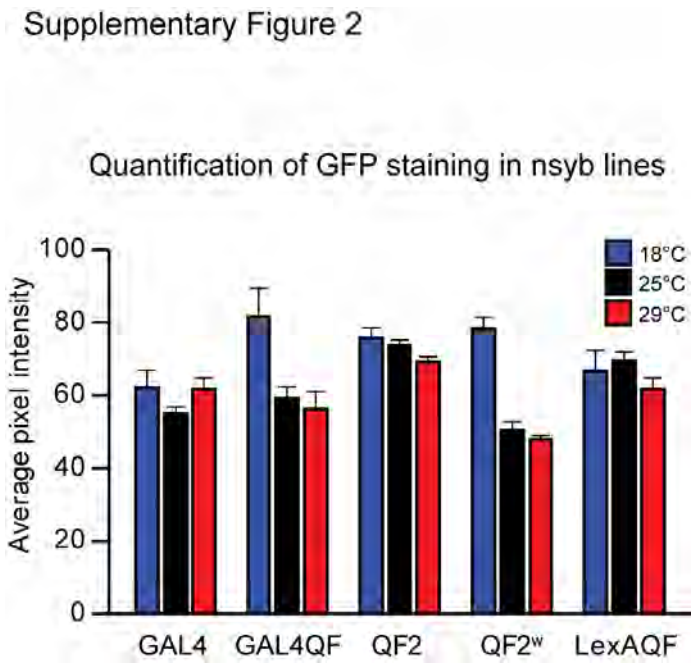

Supplementary Figure 2

Quantification of GFP expression driven by *nSyb* lines at 18 °C, 25 °C and 29 °C.
This experiment is analogous to the one shown in **Fig. 1f**, but instead of nuclearLacZ reporter, we used a membrane-bound GFP reporter (n=5 for all conditions). Flies were reared at the indicated temperature from embryonic stage until 4 days post-eclosion. This experiment allows us to investigate the possible variability of expression levels due to the nature of the reporter transgene. See **Online Methods** for details of quantification procedure.

Supplementary Figure 3

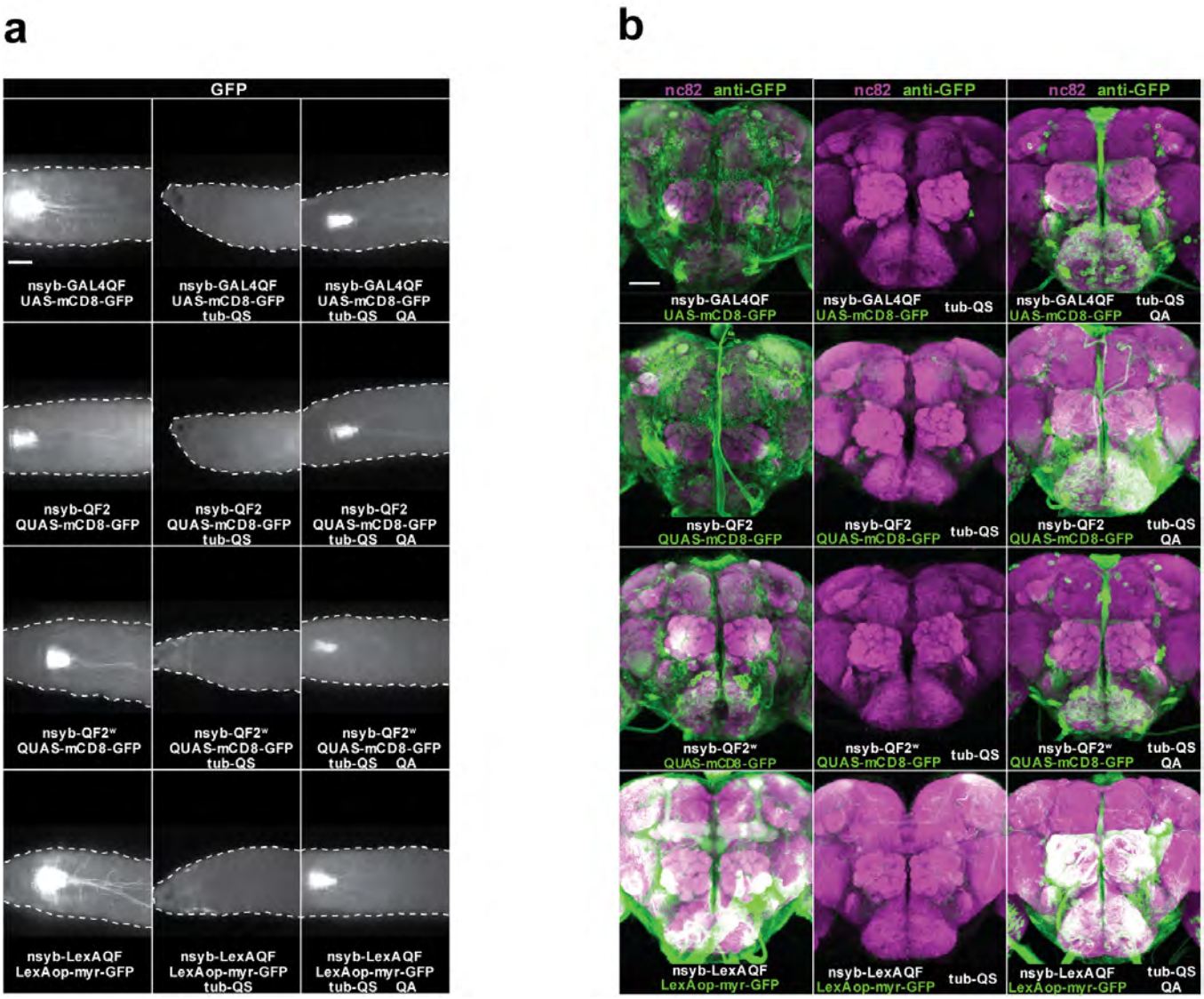

Supplementary Figure 3

Quinic acid–induced disinhibition of expression.
(a) Third instar larvae that express GFP pan-neuronally (left) have GFP expression suppressed by *tub-QS* (middle) and this suppression is inhibited by raising animals in standard fly medium supplemented by 0.1 g of quinic acid (QA) per 10 ml of food (right). All larvae are imaged at the same settings. Genotypes are indicated below corresponding images. Scale bar, 0.3 mm. **(b)** Brains of adult flies were immunostained for nc82 (magenta) and GFP (green) and imaged at the same confocal settings. To observe the effect of feeding QA to adult flies, flies were raised to adulthood on standard fly medium and transferred for 3 days into vials that contained 0.6 g of quinic acid (QA, see **Online Methods** for details). Scale bar, 50 µm.

Nature Methods: doi:10.1038/nmeth.3250

Supplementary Figure 4

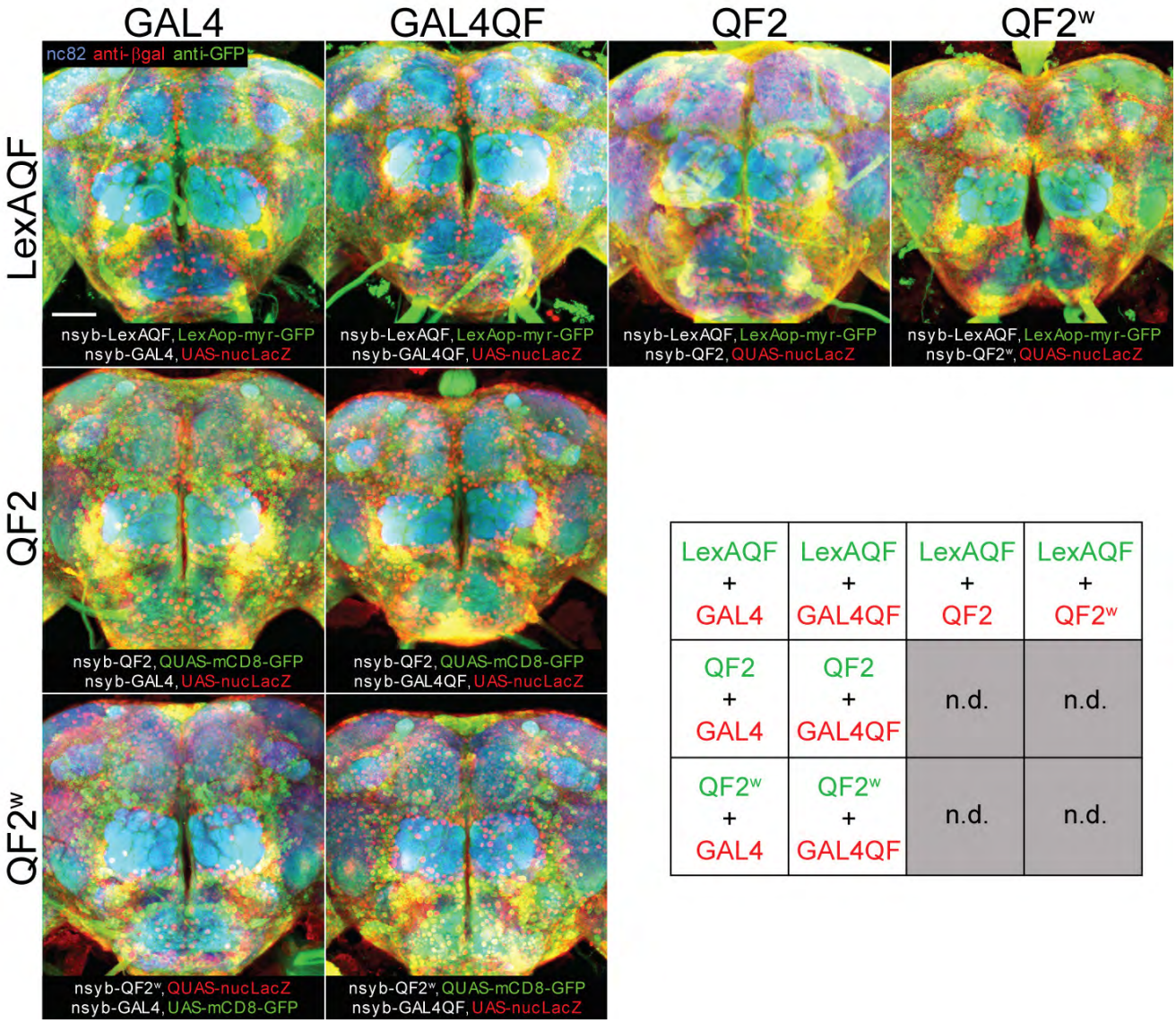

LexAQF + GAL4	LexAQF + GAL4QF	LexAQF + QF2	LexAQF + QF2^{w}
QF2 + GAL4	QF2 + GAL4QF	n.d.	n.d.
QF2^{w} + GAL4	QF2^{w} + GAL4QF	n.d.	n.d.

Supplementary Figure 4

Coexpression of *nsyb* transactivator driver lines results in viable flies that exhibit robust transgene expression.

Shown are brains of flies that carry two *nsyb* driver lines, one of which drives pan-neuronal expression of nuclear lacZ (red), and the other drives independent pan-neuronal expression of a membrane-bound GFP (green). Brains are counter-stained with nc82 (blue). *nsyb-QF2* and *nsyb-QF2^{w}* lines both drive expression of *QUAS* effectors, making it impossible to use these two drivers independently in the same cell. The same applies for *nsyb-GAL4* and *nsyb-GAL4QF* lines which both activate *UAS* effectors. All tested binary combinations yielded healthy animals, suggesting that at least two independent binary systems can be simultaneously utilized in neuronal tissues. Scale bar, 50 µm.

Supplementary Figure 5

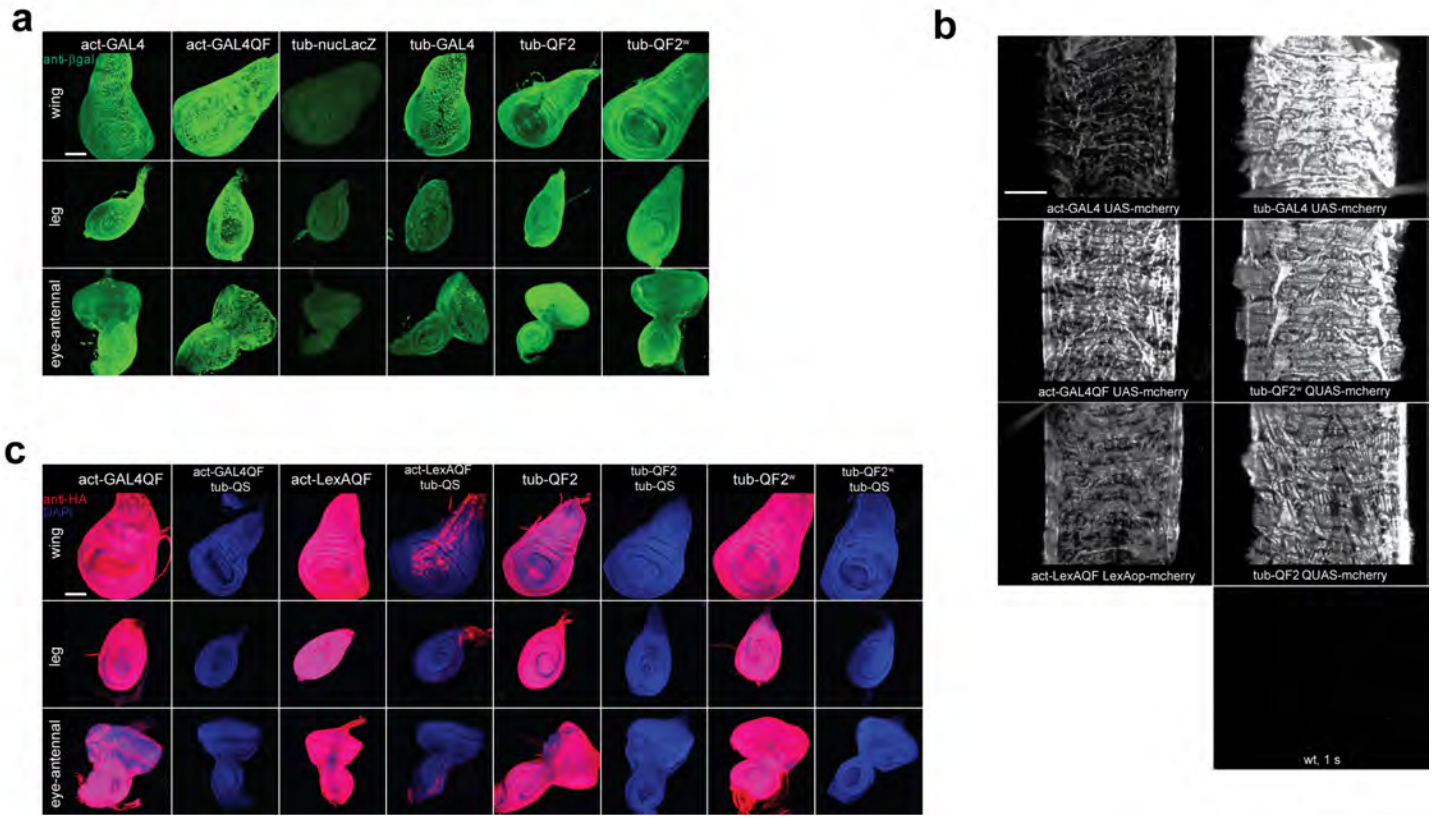

Supplementary Figure 5

Activity of ubiquitously driven QF2, QF2^{w}, GAL4QF and LexAQF in non-neuronal tissue.
(a) Expression patterns of *actin-GAL4QF*, *tubulin-QF2* and *tubulin-QF2^{w}*, visualised with a *UAS/QUAS-nuclacZ* reporter and compared to expression patterns of direct driver *tub-nucLacZ* (Bloomington stock #29726), *actin-GAL4* (Bloomington stock #3954), and *tubulin-GAL4* (Bloomington stock #5138). We did not investigate the activity of actin-LexAQF in the same way due to the unavailability of a LexAop-nuclacZ reporter. *Tubulin-nucLacZ* expression serves as a control for binary system independent expression achievable by the *tubulin* promoter. Scale bar, 50 µm. **(b)** Expression patterns represented by ubiquitous GALQF, QF2, QF2^{w} and LexAQF activity in larval body wall muscles. Each driver line was crossed to a corresponding strong hexameric mCherry reporter, as indicated on the figure panel. Third-instar larvae were dissected using the "larval fillet" preparation and imaged directly, without immunostaining, under identical illumination and image acquisition parameters for 150 ms. Wild-type control larvae were imaged for 1000 ms and produced no discernible image. Scale bar, 300 µm. **(c)** Expression and QS-mediated repression of GALQF, QF2, QF2^{w} and LexAQF activity in larval imaginal discs. Discs from larva that carried a driver and a reporter line (*actin-GAL4QF* + *5xUAS-mtdt-3HA*, *actin-LexAQF* + *13xLexAop2-6xmcherry-HA*, *tubulin-QF2* + *5xQUAS-mtdt-3HA* or *tubulin-QF2^{w}* + *5xQUAS-mtdt-3HA*) are shown in columns 1, 3, 5 and 7, correspondingly. Columns to the right of these (2, 4, 6 and 8) show imaginal discs from larvae that also carried a *tubulin-QS* transgene. All discs were immunostained for the HA epitope and counterstained with DAPI using the same protocol (see *Online Methods*). Weak residual signal in *actin-LexAQF* + *13xLexAop2-6xmcherry-HA+tub-QS* (fourth column) is observed in peripodial membrane cells. Scale bar, 50 µm.

Supplementary Note

Equipment and settings

- **Fig. 1c-d, Supplementary Fig. 1b (right column)**, confocal images of adult fly brains:
  Image size: x: 512 px, y: 512 px, z: 74 images, channels: 3, 8-bit
  Dimensions: x: 319.46 μm, y: 319.46 μm, z: 172.73 μm
  Fluorochromes: Alexa488 goat @ mouse, imaged with a 488 nm laser
  Cy3 goat @ rabbit, imaged with a 555 nm laser
  633 goat @ rat, imaged with a 639 nm laser
  Images were processed in ImageJ as follows:
  Image-> Color-> Split channels
  Plugins -> Biorad ->GJ RGB Merge (pseudocolor as follows: Alexa488 -> blue channel, Cy3 ->green channel, 633 -> red channel)
  Make one image: Image -> Stacks-> Z-project (maximum intensity projection)
  File -> Save as -> Tiff
  The figure was assembled in Adobe Illustrator, where the size of the *.tiff file was reduced as required.
- **Fig. 1e, Supplementary Fig. 1b (middle column), Supplementary Fig. 1d, Supplementary Fig. 3b**, confocal images of adult fly brains:
  Image size: x: 512 px, y: 512 px, z: 74 images, channels: 2, 8-bit
  Dimensions: x: 319.46 μm, y: 319.46 μm, z: 172.73 μm
  Fluorochromes: Alexa488 goat @ rabbit, imaged with a 488 nm laser
  Cy3 goat @ mouse, imaged with a 555 nm laser
  Images were processed in ImageJ as follows:
  Image-> Color-> Split channels
  Plugins -> Biorad ->GJ RGB Merge (pseudocolor as follows: Alexa488 -> green channel, Cy3 ->blue channel and red channel)
  Make one image: Image -> Stacks-> Z-project (maximum intensity projection)
  File -> Save as -> Tiff
  The figure was assembled in Adobe Illustrator, where the size of the *.tiff file was reduced as required.
- **Fig. 1c-e, Fig. 2a, Supplementary Fig. 3a**, **Supplementary Fig. 5b**, wide-field images of third instar larvae:
  Image size: x: 680 px; y: 512 px, 8 bit
  Dimensions: x: 2 mm; y: 1.5 mm
  Images were acquired as described in **Online Methods** ("Whole-animal imaging") and cropped/reduced in size as required in Adobe Photoshop and Adobe Illustrator.
- **Fig 2a**, wide-filed images of adult flies:
  Image size: x: 680 px; y: 512 px, 8 bit
  Dimensions: x: 7.2 mm; y: 5.4 mm
  Images were acquired as described in **Online Methods** ("Whole-animal imaging") and cropped/reduced in size as required in Adobe Photoshop and Adobe Illustrator.
- **Fig 2b**, SEM images of fly eye:
  Image size: x: 1024 px; y: 768 px, 8 bit
  Dimensions: x: 565 μm; y: 400 μm

Images were acquired as described in **Online Methods** ("Scanning electron microscopy imaging") and cropped/reduced in size as required in Adobe Photoshop and Adobe Illustrator.

- **Fig. 2b, Supplementary Fig. 5a**, confocal images of eye-antennal imaginal discs:
  Image size: x: 512 px, y: 512 px, z: 42 images, channels: 2, 8-bit
  Dimensions: x: 511 μm, y: 511 μm, z: 41 μm
  Fluorochromes: Alexa488 goat @ rabbit, imaged with a 488 nm laser
  DAPI, imaged with a 405 nm laser
  Images were processed in ImageJ as follows:
  Image-> Color-> Split channels
  Plugins -> Biorad ->GJ RGB Merge (pseudocolor as follows: Alexa488 -> green channel, DAPI ->blue channel)
  Make one image: Image -> Stacks-> Z-project (maximum intensity projection)
  File -> Save as -> Tiff
  The figure was assembled in Adobe Illustrator, where the size of the *.tiff file was reduced as required.
- **Supplementary Fig. 4**, confocal images of adult fly brains:
  Image size: x: 512 px, y: 512 px, z: 74 images, channels: 3, 8-bit
  Dimensions: x: 319.46 μm, y: 319.46 μm, z: 172.73 μm
  Fluorochromes: Alexa488 goat @ chicken (top row) or rat (middle and bottom row), imaged with a 488 nm laser
  Cy3 goat @ mouse, imaged with a 555 nm laser
  633 goat @ rabbit, imaged with a 639 nm laser
  Images were processed in ImageJ as follows:
  Image-> Color-> Split channels
  Plugins -> Biorad ->GJ RGB Merge (pseudocolor as follows: Cy3 -> blue channel, Alexa488 ->green channel, 633 -> red channel)
  Make one image: Image -> Stacks-> Z-project (maximum intensity projection)
  Increase brightness: Image -> Adjust -> Brightness/Contrast
  File -> Save as -> Tiff
  The figure was assembled in Adobe Illustrator, where the size of the *.tiff file was reduced as required.
- **Supplementary Fig. 5c**, confocal images of eye-antennal imaginal discs:
  Image size: x: 512 px, y: 512 px, z: 42 images, channels: 2, 8-bit
  Dimensions: x: 511 μm, y: 511 μm, z: 41 μm
  Fluorochromes: Cy3 goat @ rat, imaged with a 555 nm laser
  DAPI, imaged with a 405 nm laser
  Images were processed in ImageJ as follows:
  Image-> Color-> Split channels
  Plugins -> Biorad ->GJ RGB Merge (pseudocolor as follows: Cy3 -> red channel, DAPI ->blue channel)
  Make one image: Image -> Stacks-> Z-project (maximum intensity projection)
  File -> Save as -> Tiff
  The figure was assembled in Adobe Illustrator, where the size of the *.tiff file was reduced as required.

Supplementary Tables

Supplementary Table 1. Activity levels of QF variants *in vitro*.

The data in this Table is graphically presented in **Fig. 1** and **Supplementary Fig. 1**. Each average value was calculated from 4-10 independent repeats. QS suppression is calculated as the ratio of average values for Relative Luciferase activity and Relative QS-suppressed activity. QF_{orig} is the original Neurospora QF codon sequence from Reference #3. *QF* in this table, and for all variants, has been re-codonized to yield average *Drosophila* expression levels (see **Online methods**).

QF variant	*Relative Luciferase activity*		*Relative QS-suppressed activity*		*QS suppression, fold*
	mean	*SEM*	*mean*	*SEM*	
GAL4	1595.00	778.70	1072.09	196.50	1.49
QF_{orig}	1935.53	775.90	6.47	1.25	299.08
QF	1754.09	549.40	19.72	3.92	88.93
GAL4QF	2208.21	927.37	2.13	0.32	1037.79
QF2	2089.33	477.67	19.51	2.51	107.10
$QF2^{w}$	685.06	44.19	2.62	0.29	261.50
LexAQF	944.72	138.53	4.55	0.49	207.77
QF_{a}	285.41	79.48	112.83	22.58	2.53
QF_{b}	3554.81	1669.77	4.67	1.04	760.60
QF_{c}	122.52	45.75	102.64	13.97	1.19
QF_{d}	872.95	271.51	512.41	48.45	1.70
QF_{e}	234.17	81.81	63.62	4.97	3.68
QF_{f}	2417.78	668.80	49.14	5.47	49.20
QF_{g}	15.67	4.34	1.00	0.06	15.60
QF_{h}	1.29	0.08	1.01	0.04	1.27
QF_{i}	1.37	0.12	1.19	0.05	1.14
QF_{j}	1.17	0.09	1.11	0.04	1.05
QF_{k}	1.30	0.09	1.06	0.06	1.23
QF_{l}	685.35	44.52	2.02	0.20	338.82

Supplementary Table 2. Functional rescue experiments by *tub-QS*.

These experiments serve as a functional test of the effectiveness of QS-induced suppression. Flies that pan-neuronally expressed temperature-sensitive *shibire* do not survive to adulthood when raised at 29˚C. Survival is completely restored in the presence of *tub-QS*. These experiments indicate that QS efficiently inhibits the transcriptional activity of QF2 and QF2^{w} in vivo.

Genotype	***Flies of listed genotype collected (% of total progeny)***	***Flies of listed genotype expected if survival was not affected (% of total progeny)***
nsyb-QF2, *QUAS-nuclacZ/QUAS-shi^{ts}* (raised at 29C)	0 (0%)	130 (33%)
tub-QS/+; *nsyb-QF2*, *QUAS-nuclacZ/QUAS-shi^{ts}* (raised at 29C)	76 (48%)	78 (50%)
nsyb-QF2^{w}, *QUAS-nuclacZ/QUAS-shi^{ts}* (raised at 29C)	0 (0%)	31 (33%)
tub-QS/+; *nsyb-QF2^{w}*, *QUAS-nuclacZ/QUAS-shi^{ts}* (raised at 29C)	35 (51%)	34 (50%)

Supplementary Table 3. Circadian rhythm phenotypes of *nsyb-QF2* and *nsyb-QF2^{w}* compared to *nsyb-Gal4* and background control flies.

nsyb-QF2/+ and *nsyb-QF2^{w}*/+ flies exhibited normal circadian rhythms under constant darkness. Period length (tau) in these flies was similar to *nsyb-Gal4*/+ and background control flies, and rhythm strength (as measured by FFT) was intact in all flies.

Genotype	***# of flies***	***% rhythmic***	***tau ± SEM***	***Relative FFT ± SEM***
w-	29	100%	23.6±0.11	0.24±0.01
nsyb-Gal4/+	28	100%	23.6±0.06	0.17±0.01
nsyb-QF2/+	20	100%	23.7±0.12	0.18±0.01
nsyb-QF2^{w}/+	21	100%	23.7±0.06	0.20±0.02

Supplementary Table 4. Primers, used in this study.

Name	Sequence
RI-G4BD-FOR	TTTAGAATTCCAACATGAAGCTACTGTCTTCTATCGAACAAGC
QF-G4DM-FOR	ATAAGAGCATTACCCGCCTCCTCATTGACTCGGCAGCTCATCATG
QF-G4AD-FOR	ACACTGGTCTGCAGCCAATTCCACTGACCCCGTCTGCTTTG
QF-G4BD-REV	GAGCGGCTTGGCCCGACGATACAGTCAACTGTCTTTGACCTTTG
QF-G4DM-REV	GTAGGAGGGAGCTCCAACTGACGCACTAATGATTGCAGCTGTTGCTG
AATII-G4AD-REV	TATAAGACGTCTATTACTCTTTTTTTGGGTTTGGTGGG
QFrcoM1-REV	TTATAGATCTTCACTTTTTGTATGTATTAATGTCGGAGAAGTTACATCCAGG
QFrcoM2-REV	TTATAGATCTTCACTGTTTGTATGTATTAATGTCGGAGAAGTTACATCCAGG
QFrco_Nhe_FOR	GCCATGGTTGACGATTTGGC
RI-QFBD-FOR	GAAGCTAGAGAATTCCAACATGCCAC
G4-QFDM-FOR	GGTCAAAGACAGTTGACTGTATCGTCGGGCCAAGCCGCTC
G4-QFAD-FOR	CAACAGCTGCAATCATTAGTGCCGTCAGTTGGAGCTCCCTCCTAC
G4-QFBD-REV	CATGATGAGCTGCCGAGTCAATGAGGAGGCGGGTAATGCTCTTATTG
G4-QFDM-REV	CAAAGCAGACGGGGTCAGTGGAATTGGCTGCAGACCAGTGTTTG
AATII-QFAD-REV	TATTTGACGTCATCACTGTTCGTATGTATTAATGTCGGAGAAG
AATII-QFADM2-REV	TATTTGACGTCTACTACTTTTTCTTTGGGTCGACATCCACAGCG
AATII-QFADM1-REV	TATTTGACGTCATCATTTCTTCTTTTTGTATGTATTAATGTCGGAGAAGTTACATC
IF_QFBD_FOR	TCGACAGCCGAATTCCAACATGCCACCCAAGC
IF_QFAD_REV	CGACGGTATCGATAGACGTCATCACTGTTCGTATGTATTAATG
IF_QFAD_QFBD_REV	GAGCTCCAACTGACGGAGGAGGCGGGTAATGC
IF_QFBD_QFAD_FOR	ATTACCCGCCTCCTCCGTCAGTTGGAGCTCCCTC
IF_QFAD_QFAD_REV	GAGCTCCAACTGACGATCTTGAACATTGATATCCTCCG
IF_QFAD_QFAD_FOR	ATCAATGTTCAAGATCGTCAGTTGGAGCTCCCTC
IF_QFAD_QFMD_REV	GAGCTCCAACTGACGCAAACCTTCGCAGGGG
IF_QFMD_QFAD_FOR	CCCTGCGAAGGTTTGCGTCAGTTGGAGCTCCCTC
IF_QFMD475_QFBD_REV	GTGCTCTCCTCCCAAGAGGAGGCGGGTAATGC
IF_QFBD_QFMD_FOR	ATTACCCGCCTCCTCTTGGGAGGAGAGCACACAATG
11L_QF262MD_QFBD_REV	CGCCAGTGGTTAGGAGGCAGGAGGAGGCGGGTAATGC
11M_QFBD_QF262MD_FOR	CAATAAGAGCATTACCCGCCTCCTCCTGCCTCCTAACCACTGGC
11M-QFAD_QFMD475_REV	GTAGGAGGGAGCTCCAACTGACGCAAACCTTCGCAGGGGG
11R_QF475MD_QFAD_FOR	GACCCCCTGCGAAGGTTTGCGTCAGTTGGAGCTCCCTC
12L_G4MD50_QFBD_REV	TCCACTTCTGTCAGATGTGCCCTAGTAACTCCCCTCTTTTTCGGC
12M_QFBD_G4MD50_FOR	TCGCCGAAAAAGAGGGGAGTTACTAGGGCACATCTGACAGAAGTG
12M_13M_QFAD_G4MD_REV	GTAGGAGGGAGCTCCAACTGACGGGTCAGTGGCACTAATGATTGC
12R_G4MD_QFAD_FOR	CTGCAATCATTAGTGCCACTGACCCGTCAGTTGGAGCTCCCTC
13L_G4MD_QFAD_REV	GCGTCGGTGAGTGCACGATCTTTCCTATTCCAGTGCCATC
13M_QFAD_G4MD_FOR	CGGATGGCACTGGAATAGGAAAGATCGTGCACTCACCGACG
14L_QFAD_LEXBD_REV	GTAGGAGGGAGCTCCAACTGACGTCCCAGCCAATCTCCG
14R_LEXBD_QFAD_FOR	CAACGGAGATTGGCTGGGACGTCAGTTGGAGCTCCCTC
15L_QFAD_G4MD_REV	GTAGGAGGGAGCTCCAACTGACGCGTAAGTGGCACCAGACTCTG
15R_G4LXMD_QFAD_FOR	GCAGAGTCTGGTGCCACTTACGCGTCAGTTGGAGCTCCCTC
IF_FOR_GAL4DBD	CAGAGACCCCGGATCCAACATGAAGCTACTGTCTTCTATCGAAC
IF_FOR_QFDBD	CAGAGACCCCGGATCCAACATGCCACCCAAGCG
IF_FOR_LEXADBD	CAGAGACCCCGGATCGAATTCCAAAATGCCACCCAAGAAG
IF_REV_GAL4AD	TCGGTTAACGCGGCCTTCCTCTTTTTTTGGGTTTGGTGGG
IF_REV_QFAD	TCGGTTAACGCGGCCTCACTGTTCGTATGTATTAATGTCGGAG
IF_REV_LEXADBD	TCGGTTAACGCGGCCGACGTCATCACTGTTCGTATGTATTAATGTC
IF_REV_GAL4QF	TCGGTTAACGCGGCCTCATTTCTTCTTTTTGTATGTATTAATGTCGG
IF_REV_QF2W	TCGGTTAACGCGGCCGCTCATTTCTTCTTTTTGTATGTATTAATGTCGGAGAAGTTAC
IF_REV_QF_F	TCGGTTAACGCGGCCCTACTTTTTCTTTGGGTCGACATCC
IF_FOR_LexAOP_LUC	ACCTGAGCTCGCTAGGCTAGCGCATGCCTGAGG
IF_REV_LexAOP_LUC	ATTCGATATCAAGCTGACGTCACTAGTGCTAGAGTCTCCGCTTAC
IF_FOR_TUB_QF2	ATCAGATCCGCGGCCCAACATGCCACCCAAGCG
IF_REV_TUB_QF2	GCAGGTCGACCTCGAGGATCTAAACGAGTTTTTAAGCAAACTCAC
IF_FOR_ACT_QF2W	CAGAGACCCCGGATCCAACATGCCACCC
IF_REV_ACT_QF2W	CATGGTCGACGGATCGCGGCCGCTCACTGTTCGTATGTATTAATGTCG
IF_FOR_ACT_GAL4QF	CAGAGACCCCGGATCCAACATGAAGCTACTGTCTTCTATC
IF_REV_ACT_GAL4QF	CGACGGATCGCGGCCGCTCATTTCTTCTTTTTGTATGTATTAATG
IF_FOR_ACT_LEXAQF	CAGAGACCCCGGATCCAAAATGCCACCCAAGAAGAAG
IF_REV_ACT_LEXAQF	CGACGGATCGCGGCCGCTCACTGTTCGTATGTATTAATGTCGGAG
IF_FOR_GMR_QF2W	TCTGAATAGGGAATTCAACATGCCACCC
IF_REV_GMR_QF2W	ATCTGTTAACGAATTCTCATTTCTTCTTTTTGTATGTATTAATG
IF_FOR_PPT_QF2	ACAAGCTAAACAATCTGCAGGAATTCCAACATGCCACCCAAG
IF_REV_PPT_QF2	ACGCAAAGCTTGGGCTGCAGTCTAGAGGTACCCTCGAGCCGCGGCCGC
IF_FOR_DSCP_QF2	TTATGCTAGCGGATCCGAGCTCGCCCGGGGATCG
IF_REV_DSCP_QF2	TGGCATGTTGGAATTCGTTTGGTATGCGTCTTGTGATTCAAAGTTGG
IF_FOR_ATTB_QF2	TTATGCTAGCGGATCCGAGCGCCGGAGTATAAATAGAGGC
IF_REV_ATTB_QF2	TGGCATGTTGGAATTCGAGAGTTCTCTTCTTGTATTCAATAATTACTTCTTGG
IF-FOR-pCasper-ActB-QF7	CAGAGACCCCGGATCCAACATGCCACCC
IF-REV-pCaspActB-QF7	CATGGTCGACGGATCGCGGCCGCTCACTGTTCGTATGTATTAATGTCG
hsp70-AscI-FOR	AAATGGCGCGCCTATCGATACCGTCGACTAAAGCC
hsp70-NotI-REV	CCTAGGCATGCTTAATTAAGGCGGC

Supplementary Table 5. Details of PCR conditions for generating chimeric constructs.

Construct	PCR template DNA	PCR primers (see Supplementary Table 4) *
pattB-synaptobrevin-GAL4-hsp70 (GAL4) (Addgene#46107)	*pGAWB*[1]	RI-G4BD-FOR AATII-G4AD-REV
pattB-synaptobrevin-1-QFBDAD-G4DM-hsp70 (QFa) (Addgene#46109)	PCR fragment 1: *pattB-tubP-QFrco* PCR fragment 2: *pGAWB* PCR fragment 3: *pattB-tubP-QFrco*	PCR fragment 1: RI-QFBD-FOR, G4-QFDB-REV PCR fragment 2: QF-G4DM-FOR, QF-GFDM-REV PCR fragment 3: G4-QFAD-FOR, AAtII-QFAD-REV Full length product: RI-QFDB-FOR, AatII-QFAD-REV
pattB-synaptobrevin-2-G4BDDM-QFAD-hsp70 (QFb) (Addgene#46110)	PCR fragment 1: *pGAWB* PCR fragment 2: *pattB-tubP-QFrco*	PCR fragment 1: RI-G4BD-FOR, QF-G4DM-REV PCR fragment 2: G4-QFAD-FOR, AatII-QFAD-REV Full length product: RI-G4BD-FOR, AatII-QFAD-REV
pattB-synaptobrevin-3-QFBD-G4DMAD-hsp70 (QFc) (Addgene#46111)	PCR fragment 1: *pattB-tubP-QFrco* PCR fragment 2: *pGAWB*	PCR fragment 1: RI-QFBD-FOR, G4-QFBD-REV PCR fragment 2: QF-G4DM-FOR, AatII-G4AD-REV Full length product: RI-QFBD-FOR, AatII-G4AD-REV
pattB-synaptobrevin-4-QFBDDM-G4AD-hsp70 (QFd) (Addgene#46112)	PCR fragment 1: *pGAWB* PCR fragment 2: *pattB-tubP-QFrco*	PCR fragment 1: QF-G4AD-FOR, AatII-G4AD-REV PCR fragment 2: RI-QFBD-FOR, G4-QFDM-REV Full length product: RI-QFBD-FOR, AatII-G4AD-REV
pattB-synaptobrevin-5-G4BDDM-QFADM1-hsp70 (GAL4QF) (Addgene#46113)	PCR fragment 1: *pGAWB* PCR fragment 2: *pattB-tubP-QFrcoM1*	PCR fragment 1: RI-G4BD-FOR, QF-G4DM-REV PCR fragment 2: G4-QFAD-FOR, AatII-QFADM1-REV Full length product: RI-G4BD-FOR, AatII-QFADM1-REV
pattB-synaptobrevin-6-G4BDDM-QFADM2-hsp70 (QFe) (Addgene#46114)	PCR fragment 1: *pGAWB* PCR fragment 2; *pattB-tubP-QFrco*	PCR fragment 1: RI-G4BD-FOR, QF-G4DM-REV PCR fragment 2: G4-QFAD-FOR, AatII-QFADM2-REV Full length products RI-G4BD-FOR, AatII-QFADM2-REV
pattB-synaptobrevin-7-QFBDAD-hsp70 (QF2) (Addgene#46115)	PCR fragment 1: *pattB-tubP-QFrco* PCR fragment 2: *pattB-tubP-QFrco*	PCR fragment 1: IF-QFBD-FOR, IF-QFAD-QFBD-REV PCR fragment 2: IF-QFBD-QFAD-FOR, IF-QFAD-REV Full length product: IF-QFBD-FOR, IF-QFAD-REV
pattB-synaptobrevin-8-QFAD184-214-hsp70 (QFf) (Addgene#46117)	PCR fragment 1: *pattB-tubP-QFrco* PCR fragment 2: *pattB-tubP-QFrco*	PCR fragment 1: IF-QFBD-FOR, IF-QFAD-QFAD-REV PCR fragment 2: IF-QFAD-QFAD-FOR, IF-QFAD-REV Full length product: IF-QFBD-FOR, IF-QFAD-REV
pattB-synaptobrevin-9-QFMD184-475-hsp70 (QFg) (Addgene#46118)	PCR fragment 1: *pattB-tubP-QFrco* PCR fragment 2: *pattB-tubP-QFrco*	PCR fragment 1: IF-QFBD-FOR, IF-QFAD-QFMD-REV PCR fragment 2: IF-QFMD-QFAD-FOR, IF-QFAD-REV Full length product: IF-QFBD-FOR, IF-QFAD-REV
pattB-synaptobrevin-10-QFMD475-650-hsp70 (QFh) (Addgene#46119)	PCR fragment 1: *pattB-tubP-QFrco* PCR fragment 2: *pattB-tubP-QFrco*	PCR fragment 1: IF-QFBD-FOR, IF-QFMD475-QFBD-REV PCR fragment 2: IF-QFBD-QFMD-FOR, IF-QFAD-REV Full length product: IF-QFBD-FOR, IF-QFAD-REV
pattB-synaptobrevin-11-QFMD262-475-hsp70 (QFi) (Addgene#46120)	PCR fragment 1: *pattB-tubP-QFrco* PCR fragment 2: *pattB-tubP-QFrco* PCR fragment 3: *pattB-tubP-QFrco*	PCR fragment 1: IF-QFBD-FOR, 11L_QF262MD_QFBD_REV PCR fragment 2: 11M_QFBD_QF262MD_FOR, 11M-QFAD_QFMD475_REV PCR fragment 3: 11R_QF475MD_QFAD_FOR, IF-QFAD-REV Full length product: IF-QFBD-FOR, IF-QFAD-REV
pattB-synaptobrevin-12-QFBDAD-G4DM50-761-hsp70 (QFj) (Addgene#46121)	PCR fragment 1: *pattB-tubP-QFrco* PCR fragment 2: *pGaWB* PCR fragment 3: *pattB-tubP-QFrco*	PCR fragment 1: IF-QFBD-FOR, 12L-G4MD50-QFBD-REV PCR fragment 2: 12M-QFBD-G4MD50-FOR, 12M_13M-QFAD-G4MD-REV PCR fragment 3: 12R-G4MD-QFAD-FOR, IF-QFAD-REV Full length product: IF-QFBD-FOR, IF-QFAD-REV
pattB-synaptobrevin-13-QFBDAD-G4MD257-761-hsp70 (QFk) (Addgene#46122)	PCR fragment 1: *pattB-tubP-QFrc* PCR fragment 2: *pGaWB* PCR fragment 3: *pattB-tubP-QFrco*	PCR fragment 1: IF-QFBD-FOR, 13L-G4MD-QFAD-REV PCR fragment 2: 13M-QFAD-G4MD-FOR, 12M_13M-QFAD-G4MD-REV PCR fragment 3: 13R-G4MD-QFAD-FOR, IF-QFAD-REV Full length product: IF-QFBD-FOR, IF-QFAD-REV
pattB-synaptobrevin-14-LexA-QF-hsp70 (LexAQF)	PCR fragment 1: *pBPnlsLexA::GADflUw*[24] (Addgene#26232)	PCR fragment 1: IF-LEXBD-FOR, 14L-QFAD-LEXBD-REV PCR fragment 2: 14R-LEXBD-QFAD-FOR, IF-QFAD-REV Full length product: IF-LEXBD-FOR, IF-QFAD-REV

(Addgene#46123)	PCR fragment 2: *pattB-tubP-QFrco*	
pattB-synaptobrevin-15-LexABD-G4MD-QFAD-hsp70 (LexAG4QF) (Addgene#46124)	PCR fragment 1: *pBPnlsLexA::GADflUw* PCR fragment 2: *pattB-tubP-QFrco*	PCR fragment 1: IF-LEXBD-FOR, 15L-QFAD-G4MD-REV PCR fragment 2: 15R-G4LXMD-QFAD-FOR, IF-QFAD-REV Full length product: IF-LEXBD-FOR, IF-QFAD-REV
pattB-synaptobrevin-QF2w-hsp70 (QF2w) (Addgene#46116)	pAC-QF2w	RI-QFBD-FOR, AatII-QFADM1-REV

* For PCR reactions with 2 fragments, PCR fragments 1 and 2 were incubated in a PCR reaction for 5 cycles and external oligos included for another 25 cycles. For PCR reactions with 3 fragments, PCR fragments 1 and 2 were incubated in a PCR reaction for 5 cycles, and in a separate PCR reaction, PCR fragments 2 and 3 were incubated together for 5 cycles. These two separate reactions were then mixed, cycled 5 times, and external oligos included for another 25 cycles.